Supplementary Information

Next-Generation *in Situ* Hybridization Chain Reaction: Higher Gain, Lower Cost, Greater Durability

Harry M.T. Choi[1], Victor A. Beck[1], and Niles A. Pierce[1,2,*]

[1]Division of Biology & Biological Engineering, [2]Division of Engineering & Applied Science,
California Institute of Technology, Pasadena, CA 91125, USA

[*]Email: niles@caltech.edu

Contents

S1 Protocols

S1.1 Preparation of fixed whole-mount zebrafish embryos

1. Collect embryos and incubate at 28 °C in a petri dish with egg H_2O until they reach 20 h post-fertilization (20 hpf).
2. Dechorinate using two pairs of sharp tweezers under a dissecting scope.
3. Transfer ∼80 embryos (27 hpf) to a 2 mL eppendorf tube and remove excess egg H_2O.
4. Fix embryos in 1 mL of 4% paraformaldehyde (PFA)* for 24 h at 4 °C.
5. Wash embryos 3 × 5 min with 1 mL of 1× phosphate-buffered saline (PBS) to stop the fixation. Fixed embryos can be stored at 4 °C at this point.
6. Dehydrate and permeabilize with a series of methanol (MeOH) washes (1 mL each):
   (a) 100% MeOH for 4 × 10 min
   (b) 100% MeOH for 1 × 50 min.
7. Rehydrate with a series of graded 1 mL MeOH/PBST washes for 5 min each:
   (a) 75% MeOH / 25% PBST
   (b) 50% MeOH / 50% PBST
   (c) 25% MeOH / 75% PBST
   (d) 5 × 100% PBST.
8. Store embryos at 4 °C before use.†

*Use fresh PFA and cool to 4 °C before use to avoid increased autofluorescence.
†Prepare embryos every two weeks to avoid increased autofluorescence.

S1.2 Buffer recipes for embryo preparation

10× PBS[‡]	For 1 L of solution
1.37 M NaCl	80 g NaCl
27 mM KCl	2 g KCl
80 mM Na_2HPO_4	11.4 g Na_2HPO_4 anhydrous
20 mM KH_2PO_4	2.7 g KH_2PO_4 anhydrous
pH 7.4	Adjust pH to 7.4 with HCl
	Fill up to 1 L with ultrapure H_2O

4% Paraformaldehyde (PFA)	For 25 mL of solution
4% PFA	1 g of PFA powder
1× PBS	25 mL of 1× PBS

PBST	For 50 mL of solution
1× PBS	5 mL of 10× PBS
0.1% Tween 20	500 μL of 10% Tween 20
	Fill up to 50 mL with ultrapure H_2O

[‡] Avoid using calcium chloride and magnesium chloride in PBS as this leads to increased autofluorescence in the embryos.

S1.3 Two-stage multiplexed *in situ* hybridization using RNA HCR

Detection stage

1. For each sample, move 8 embryos to a 1.5 mL eppendorf tube.
2. Pre-hybridize with 350 μL of 50% hybridization buffer (50% HB) for 30 min at 55 °C.
3. Prepare probe solution by adding 6 pmol of each probe (1 μL of 6 μM stock per probe) to 500 μL of 50% HB at 55 °C.
4. Remove the pre-hybridization solution and add the probe solution.
5. Incubate the embryos overnight (12–16 h) at 55 °C.
6. Remove excess probes by washing at 55 °C with 500 μL of:
   (a) 75% of 50% HB / 25% 2× SSCT for 15 min
   (b) 50% of 50% HB / 50% 2× SSCT for 15 min
   (c) 25% of 50% HB / 75% 2× SSCT for 15 min
   (d) 100% 2× SSCT for 15 min
   (e) 100% 2× SSCT for 30 min.

   Wash solutions should be pre-heated to 55 °C before use.

Amplification stage

1. Pre-amplify embryos with 350 μL of 40% HB for 30 min at 45 °C.
2. Prepare 30 pmol of each fluorescently labeled hairpin by snap cooling in 10 μL of 1× TE with 150 mM NaCl (heat at 95 °C for 90 seconds and cool to room temperature on the benchtop for 30 min).
3. Prepare hairpin solution by adding all snap-cooled hairpins to 500 μL of 40% HB at 45 °C.
4. Remove the pre-amplification solution and add the hairpin solution.
5. Incubate the embryos overnight (12–16 h) at 45 °C.
6. Repeat step 6 above using 40% HB at 45 °C (instead of 50% HB at 55 °C).
7. Wash at room temperature for 10 min with 500 μL of 2× SSCT.

S1.4 Buffer recipes for RNA HCR

50% Hybridization buffer (50% HB)	For 40 mL of solution
50% formamide	20 mL formamide
2× sodium chloride sodium citrate (SSC)	4 mL of 20× SSC
9 mM citric acid (pH 6.0)	360 μL 1 M citric acid, pH 6.0
0.1% Tween 20	400 μL of 10% Tween 20
500 μg/mL tRNA	200 μL of 100 mg/mL tRNA
50 μg/mL heparin	200 μL of 10 mg/mL heparin
	Fill up to 40 mL with ultrapure H_2O

40% Hybridization buffer (40% HB)	For 40 mL of solution
40% formamide	16 mL formamide
2× sodium chloride sodium citrate (SSC)	4 mL of 20× SSC
9 mM citric acid (pH 6.0)	360 μL 1 M citric acid, pH 6.0
0.1% Tween 20	400 μL of 10% Tween 20
500 μg/mL tRNA	200 μL of 100 mg/mL tRNA
50 μg/mL heparin	200 μL of 10 mg/mL heparin
	Fill up to 40 mL with ultrapure H_2O

2× SSCT	For 40 mL of solution
2× sodium chloride sodium citrate (SSC)	4 mL of 20× SSC
0.1% Tween 20	400 μL of 10% Tween 20
	fill up to 40 mL with ultrapure H_2O

S1.5 Two-stage multiplexed *in situ* hybridization using DNA HCR

Detection stage

1. For each sample, move 8 embryos to a 1.5 mL eppendorf tube.
2. Pre-hybridize with 350 μL of probe hybridization buffer for 30 min at 45 °C.
3. Prepare probe solution by adding 1 pmol of each probe (1 μL of 1 μM stock per probe) to 500 μL of probe hybridization buffer at 45 °C.
4. Remove the pre-hybridization solution and add the probe solution.
5. Incubate the embryos overnight (12–16 h) at 45 °C.
6. Remove excess probes by washing at 45 °C with 500 μL of:
   (a) 75% of probe wash buffer / 25% 5× SSCT for 15 min
   (b) 50% of probe wash buffer / 50% 5× SSCT for 15 min
   (c) 25% of probe wash buffer / 75% 5× SSCT for 15 min
   (d) 100% 5× SSCT for 15 min
   (e) 100% 5× SSCT for 30 min.

   Wash solutions should be pre-heated to 45 °C before use.

Amplification stage

1. Pre-amplify embryos with 350 μL of amplification buffer for 30 min at room temperature.
2. Prepare 30 pmol of each fluorescently labeled hairpin by snap cooling in 10 μL of 5× SSC buffer (heat at 95 °C for 90 seconds and cool to room temperature on the benchtop for 30 min).
3. Prepare hairpin solution by adding all snap-cooled hairpins to 500 μL of amplification buffer at room temperature.
4. Remove the pre-amplification solution and add the hairpin solution.
5. Incubate the embryos overnight (12–16 h) at room temperature.
6. Remove excess hairpins by washing with 500 μL of 5× SSCT at room temperature:
   (a) 2 × 5 min
   (b) 2 × 30 min
   (c) 1 × 5 min

S1.6 Buffer recipes for DNA HCR

Probe hybridization buffer	For 40 mL of solution
50% formamide	20 mL formamide
5× sodium chloride sodium citrate (SSC)	10 mL of 20× SSC
9 mM citric acid (pH 6.0)	360 μL 1 M citric acid, pH 6.0
0.1% Tween 20	400 μL of 10% Tween 20
50 μg/mL heparin	200 μL of 10 mg/mL heparin
1× Denhardt's solution	800 μL of 50× Denhardt's solution
10% dextran sulfate	8 mL of 50% dextran sulfate
	Fill up to 40 mL with ultrapure H_2O

Probe wash buffer	For 40 mL of solution
50% formamide	20 mL formamide
5× sodium chloride sodium citrate (SSC)	10 mL of 20× SSC
9 mM citric acid (pH 6.0)	360 μL 1 M citric acid, pH 6.0
0.1% Tween 20	400 μL of 10% Tween 20
50 μg/mL heparin	200 μL of 10 mg/mL heparin
	Fill up to 40 mL with ultrapure H_2O

Amplification buffer	For 40 mL of solution
5× sodium chloride sodium citrate (SSC)	10 mL of 20× SSC
0.1% Tween 20	400 μL of 10% Tween 20
10% dextran sulfate	8 mL of 50% dextran sulfate
	Fill up to 40 mL with ultrapure H_2O

5× SSCT	For 40 mL of solution
5× sodium chloride sodium citrate (SSC)	10 mL of 20× SSC
0.1% Tween 20	400 μL of 10% Tween 20
	fill up to 40 mL with ultrapure H_2O

50% dextran sulfate	For 40 mL of solution
50% dextran sulfate	20 g of dextran sulfate powder
	Fill up to 40 mL with ultrapure H_2O

S1.7 Reagents and supplies

Alexa Fluor 488 carboxylic acid, 2,3,5,6-tetrafluorophenyl ester (Molecular Probes Cat. # A-30005)
Alexa Fluor 514 carboxylic acid, succinimidyl ester (Molecular Probes Cat. # A-30002)
Alexa Fluor 546 carboxylic acid, succinimidyl ester (Molecular Probes Cat. # A-20002)
Alexa Fluor 647 carboxylic acid, succinimidyl ester (Molecular Probes Cat. # A-20006)
Alexa Fluor 700 carboxylic acid, succinimidyl ester (Molecular Probes Cat. # A-20010)
N,N-Dimethlyformamide (DMF) (Alfa Aesar Cat. # 43997-AE)
Paraformaldehyde (PFA) (Sigma Cat. # P6148)
Formamide (Deionized) (Ambion Cat. # AM9342)
20$\times$ sodium chloride sodium citrate (SSC) (Invitrogen Cat. # 15557-044)
Heparin (Sigma Cat. # H3393)
50% Tween 20 (Invitrogen Cat. # 00-3005)
50$\times$ Denhardt's solution (Invitrogen Cat. # 750018)
Dextran sulfate (Sigma Cat. # D6001)
25 mm $\times$ 75 mm glass slide (VWR Cat. # 48300-025)
22 mm $\times$ 22 mm No. 1 coverslip (VWR Cat. # 48366-067)
SYBR Gold nucleic acid gel stain (Invitrogen Cat. # S-11494)
SlowFade Gold antifade reagent with DAPI (Molecular Probes Cat. # S36938)

S2 Non-specific hairpin binding in stringent and permissive hybridization conditions

To assess the background resulting from non-specific binding of DNA HCR hairpins *in situ*, we performed *in situ* hybridization experiments while omitting certain reagents to assess the following:

- Autofluorescence (AF): No probe, no hairpins.
- AF + non-specific hairpin binding: No probe, one hairpin (2× H1). With only one hairpin, no amplification is possible, so any augmentation of AF is attributable to non-specific hairpin binding.
- Autofluorescence + non-specific amplification (AF + NSA): No probe, both hairpins (H1 + H2). Any augmentation of AF is attributable to NSA (individual or polymerized hairpins that bind non-specifically in the sample).

Using the stringent *in situ* amplification conditions (40% formamide, 45 °C) employed for the first-generation RNA HCR *in situ* amplification technology,[1] minimal non-specific hairpin binding is observed (Fig. S1). Using previously tested permissive *in situ* amplification conditions (1× SPSC, room temperature),[2] fluorescent puncta are observed using one or both hairpins, indicating non-specific hairpin binding (Fig. S2). In the present study, we discovered new permissive *in situ* amplification conditions (5× SSCT, 10% dextran sulfate, room temperature) that eliminate the formation of fluorescent puncta arising from non-specific hairpin binding (Fig. S3). All confocal images in Figs S1–S3 were collected with the microscope gain adjusted to avoid saturating pixels using DNA HCR to map a transgenic target mRNA (row 4 of Fig. S3).

To further investigate the new permissive *in situ* amplification conditions, we performed additional studies leaving out either dextran sulfate or Tween 20 (Fig. S4), revealing that dextran sulfate appears to be primarily responsible for minimizing non-specific amplification. All confocal images in Fig. S4 were collected with the microscope gain adjusted to avoid saturating pixels using DNA HCR to map a transgenic target mRNA (column 1 of Fig. S4).

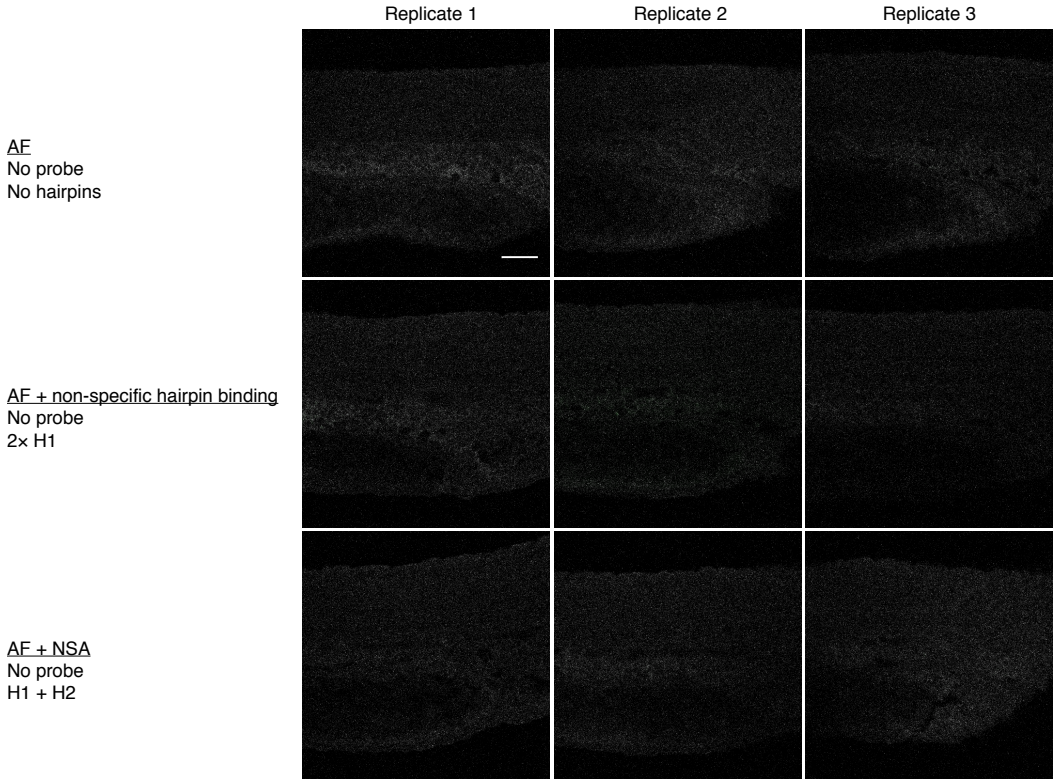

Figure S1. Non-specific binding of DNA HCR hairpins in the stringent *in situ* amplification conditions employed for the first-generation RNA HCR technology.[1] Sample: transgenic whole-mount zebrafish embryo. Green channel (excitation 633 nm): hairpin staining (HCR B4-Alexa647) plus autofluorescence. Gray channel (excitation 488 nm): autofluorescence to depict sample morphology. Experiments were performed using the RNA HCR protocol (Section S1.3) using DNA HCR hairpins. Embryos fixed: 27 hpf. Scale bar: 50 μm.

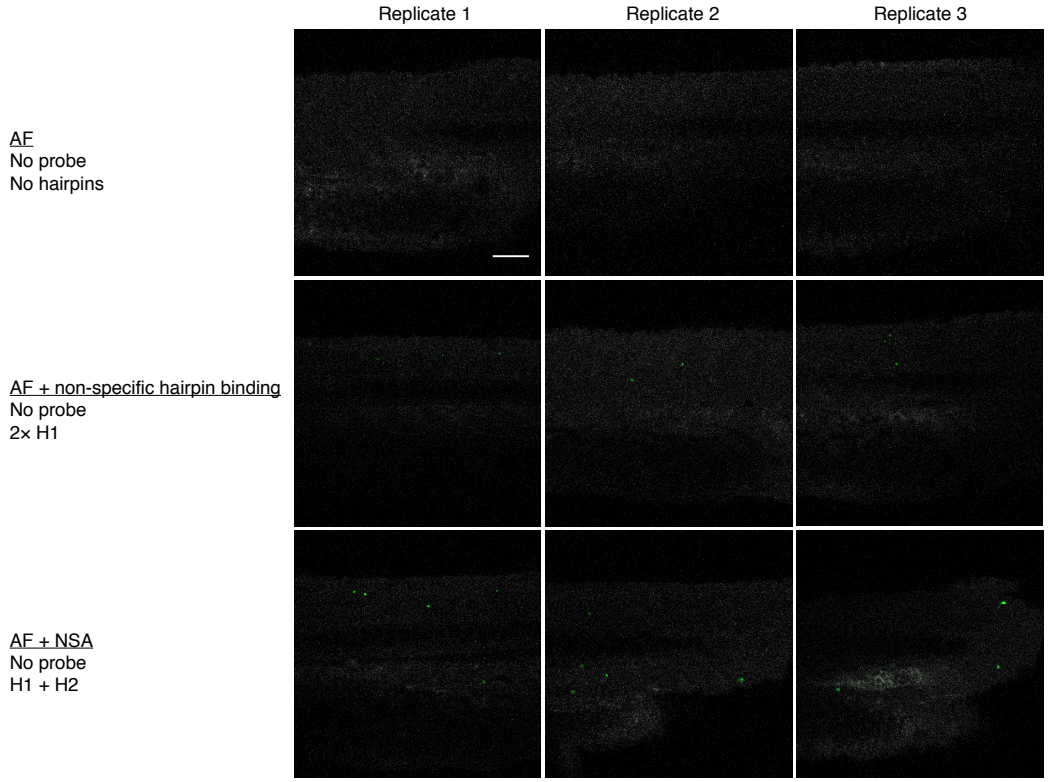

Figure S2. Non-specific binding of DNA HCR hairpins in previously studied permissive *in situ* amplification conditions.[2] Sample: transgenic whole-mount zebrafish embryo. Green channel (excitation 633 nm): hairpin staining (HCR B4-Alexa647) plus autofluorescence. Gray channel (excitation 488 nm): autofluorescence to depict sample morphology. Experiments were performed using the DNA HCR protocol (Section S1.5) substituting RNA 50% hybridization buffer (Section S1.4) as the probe hybridization buffer and $1\times$ SPSC (50 mM Na_2HPO_4, 0.5 M NaCl, pH 6.8) as the amplification buffer. Embryos fixed: 27 hpf. Scale bar: 50 μm.

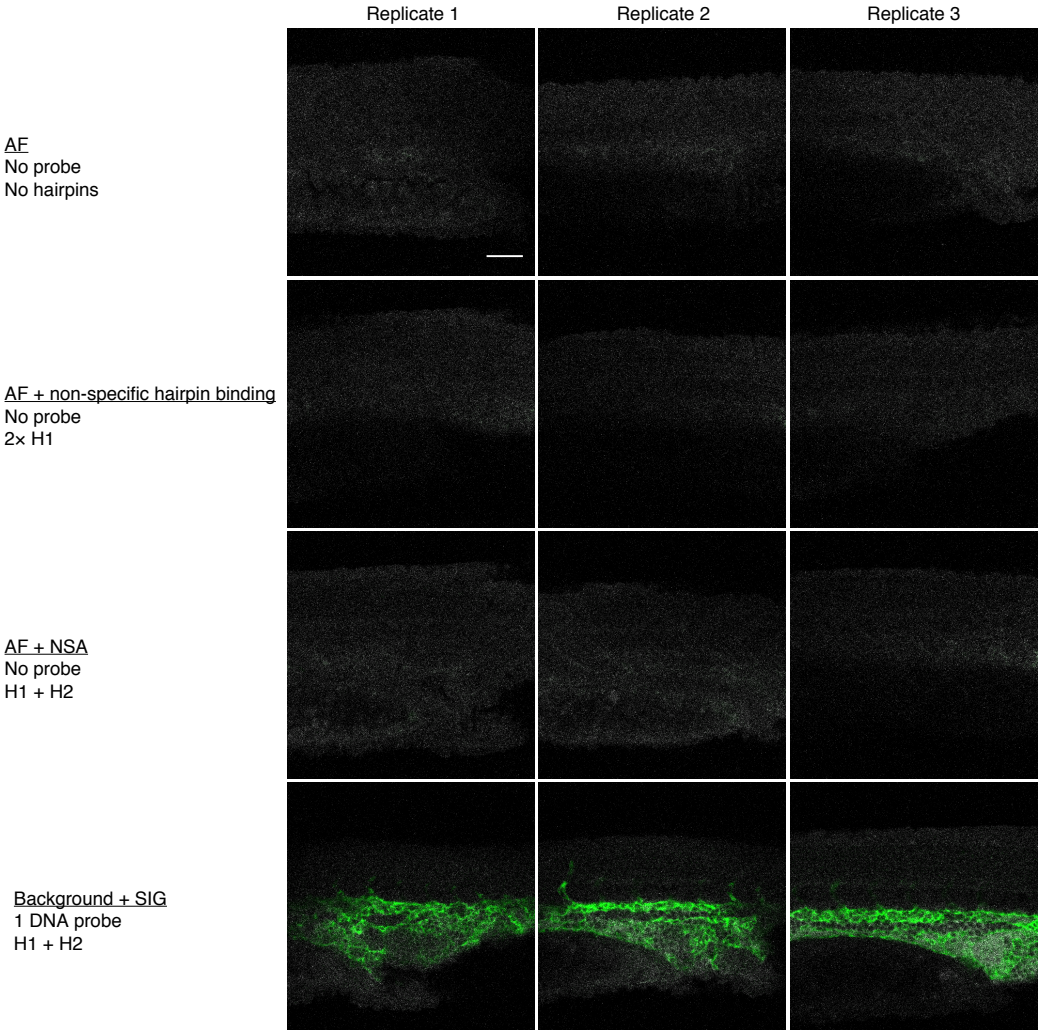

Figure S3. Non-specific binding of DNA HCR hairpins in new permissive *in situ* amplification conditions. Sample: transgenic whole-mount zebrafish embryo. Green channel (excitation 633 nm): hairpin staining (HCR B4-Alexa647) plus autofluorescence. Gray channel (excitation 488 nm): autofluorescence to depict sample morphology. Experiments were performed using the DNA HCR protocol (Section S1.5). Embryos fixed: 27 hpf. Scale bar: 50 μm.

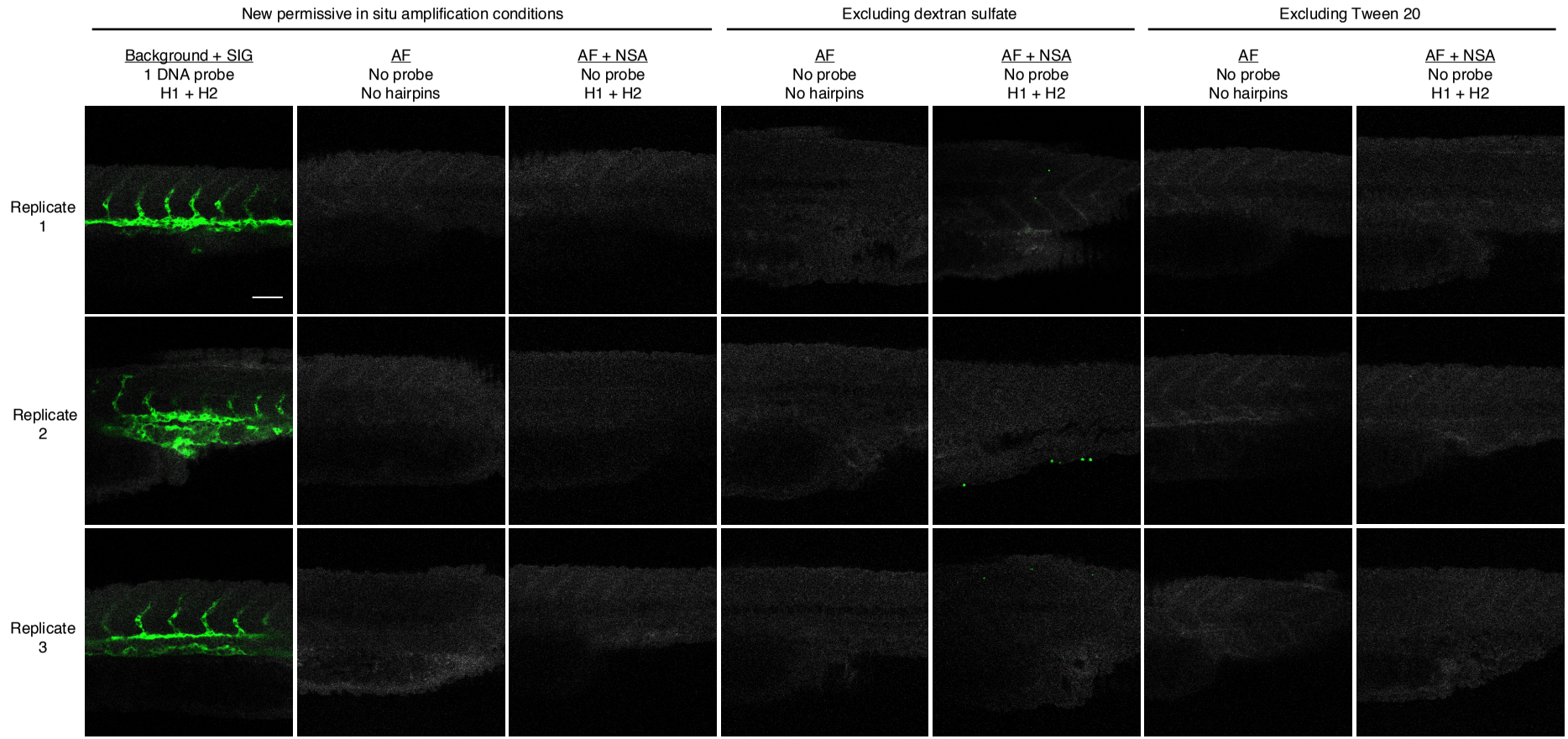

Figure S4. Non-specific amplification using DNA HCR hairpins in new permissive *in situ* amplification conditions leaving out either dextran sulfate or Tween 20. Sample: transgenic whole-mount zebrafish embryo. Green channel (excitation 633 nm): hairpin staining (HCR B4-Alexa647) plus autofluorescence. Gray channel (excitation 488 nm): autofluorescence to depict sample morphology. Experiments were performed using the DNA HCR protocol (Section S1.5) without modification (columns 1–3), or excluding dextran sulfate from the probe hybridization and amplification buffers (columns 4–5), or excluding Tween 20 from the probe hybridization, probe wash, and amplification buffers (columns 6–7). Embryos fixed: 27 hpf. Scale bar: 50 μm.

S3 *In silico* and *in vitro* analysis of DNA HCR amplifiers

Equilibrium test tube calculations were performed using the analysis feature of the NUPACK web application.[3,4] For each of five DNA HCR amplifiers, a computational stepping study was performed to check that initiators, hairpins, and polymerization intermediates were predicted to be well-formed with high yield in test tubes containing different subsets of strands (panel (a) of Figures S5–S9). Typically, initiators, hairpins, and intermediates were predicted to be well-formed with quantitative yield. The exception is amplifier B1, for which the initiators that are intended to be unstructured monomers are predicted to have some internal base-pairing and dimerization at equilibrium. These imperfections arise from the fact that B1 was designed by redimensioning an existing DNA HCR amplifier, whereas B2–B5 were designed from scratch for the present study. A computational orthogonality study was performed to check that each of the five DNA HCR amplifiers is *not* triggered by the initiators for the other four amplifiers (panel (b) of Figures S5–S9). All calculations were performed using nearest-neighbor free-energy parameters[5–7] in 0.975 M Na^+ at 25 °C to match the experimental temperature and salt conditions for DNA HCR *in situ* amplification (5× SSCT, room temperature).

Experimental test tube studies were used to validate the conditional polymerization properties of each of the five DNA HCR amplifiers (Figure S10). For each amplifier, the hairpins exhibit metastability in the absence of a cognate initiator and undergo conditional polymerization upon the introduction of a cognate initiator. Likewise, experimental test tube studies were used to validate that the five DNA HCR amplifiers operate orthogonally (Figure S11). For each amplifier, the hairpins undergo conditional polymerization upon introduction of a cognate initiator and do *not* polymerize upon introduction of the initiators for the other four amplifiers.

Our fluorescent gel scanner and fluorescent confocal microscope are suitable for detecting up to four spectrally distinct HCR amplifiers simultaneously. In the present work, we validate five orthogonal next-generation DNA HCR amplifiers to assist researchers in performing future five-channel studies using different hardware.

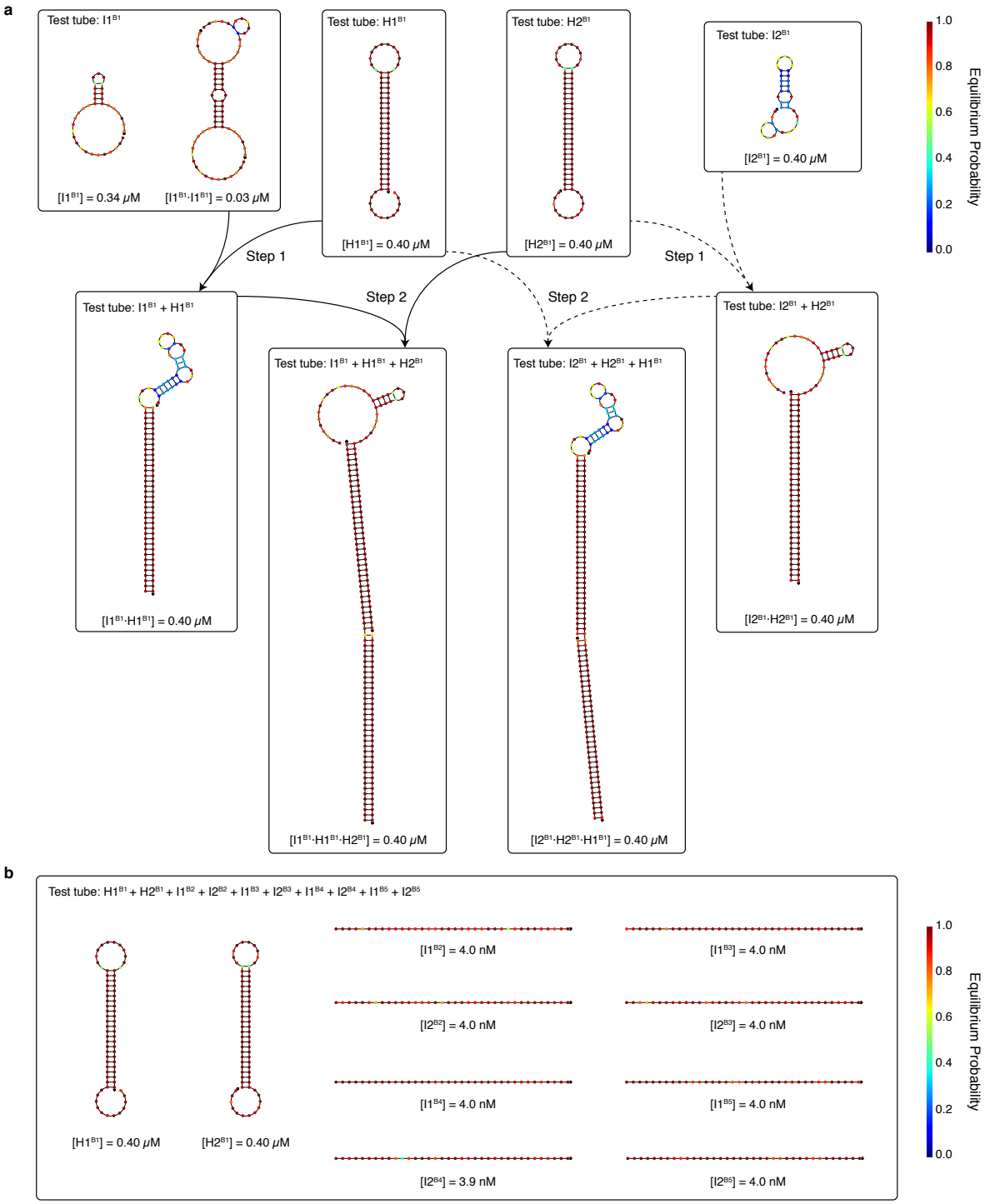

Figure S5. Computational analysis of DNA HCR amplifier B1. (a) Stepping study. Equilibrium test tube calculations showing the predicted concentrations and base-pairing properties of initiators, hairpins, and polymerization intermediates. The initiators (I1 and I2) are predicted to have some internal base-pairing and dimerization at equilibrium; hairpins and polymerization intermediates are predicted to form with quantitative yield. (b) Orthogonality study. Equilibrium test tube calculations predict that polymerization is not triggered by the initiators for the other four amplifiers. (a,b) Each box represents a test tube containing the strands listed at the top at concentrations: 0.4 μM hairpins and initiators for panel a, 0.4 μM hairpins and 4 nM initiators for panel b. For each test tube, thermodynamic analysis yields the equilibrium concentrations and base-pairing ensemble properties for all complexes containing up to three strands. Each complex predicted to form with appreciable concentration at equilibrium is depicted by its minimum free energy structure, with each nucleotide shaded by the probability that it adopts the depicted base pairing state at equilibrium. The predicted equilibrium concentration is noted below each complex.

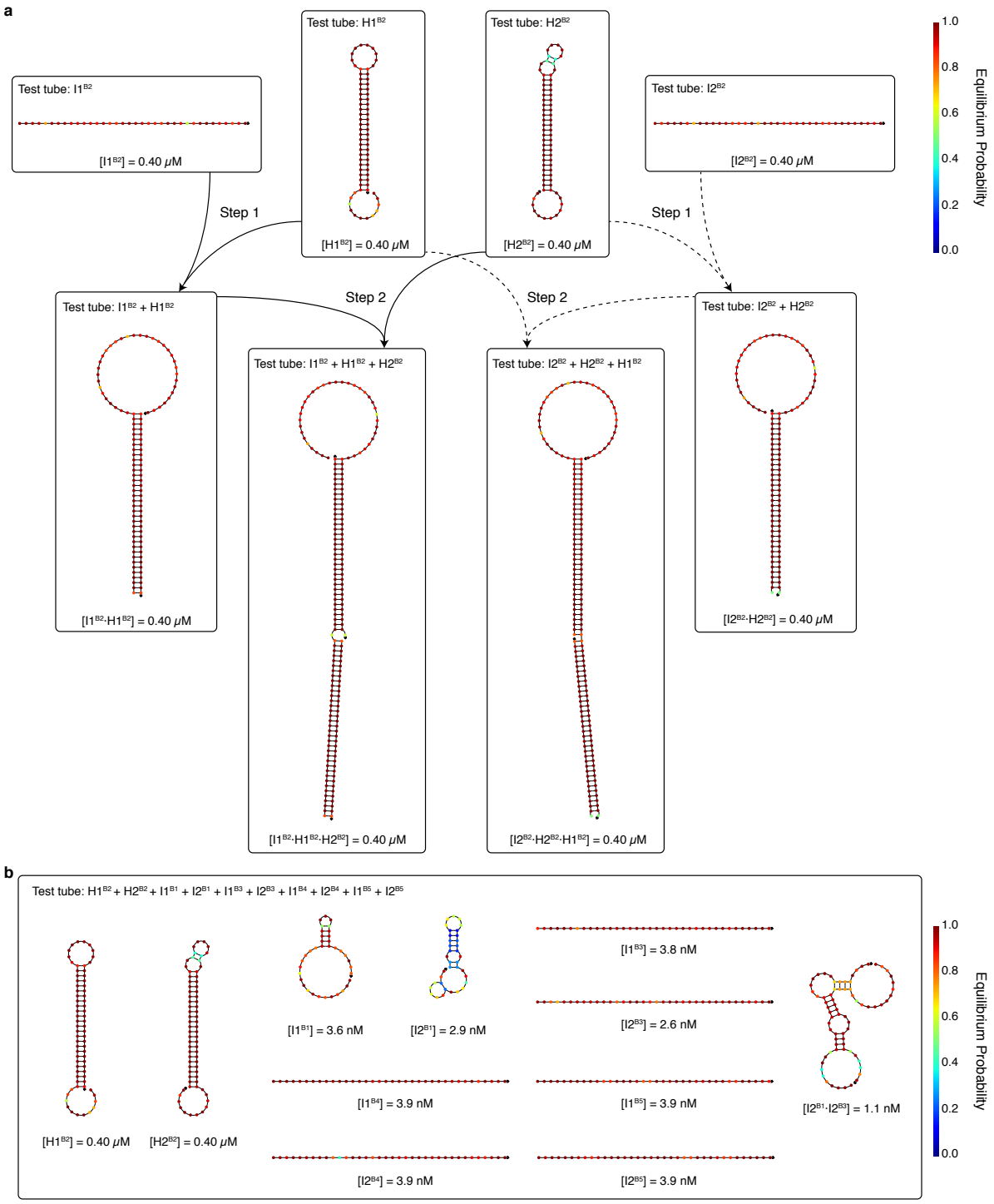

Figure S6. Computational analysis of DNA HCR amplifier B2. (a) Stepping study. Equilibrium test tube calculations predict that initiators, hairpins, and polymerization intermediates are well-formed with quantitative yield. (b) Orthogonality study. Equilibrium test tube calculations predict that polymerization is not triggered by the initiators for the other four amplifiers. (a,b) Each box represents a test tube containing the strands listed at the top at concentrations: 0.4 μM hairpins and initiators for panel a, 0.4 μM hairpins and 4 nM initiators for panel b. For each test tube, thermodynamic analysis yields the equilibrium concentrations and base-pairing ensemble properties for all complexes containing up to three strands. Each complex predicted to form with appreciable concentration at equilibrium is depicted by its minimum free energy structure, with each nucleotide shaded by the probability that it adopts the depicted base pairing state at equilibrium. The predicted equilibrium concentration is noted below each complex.

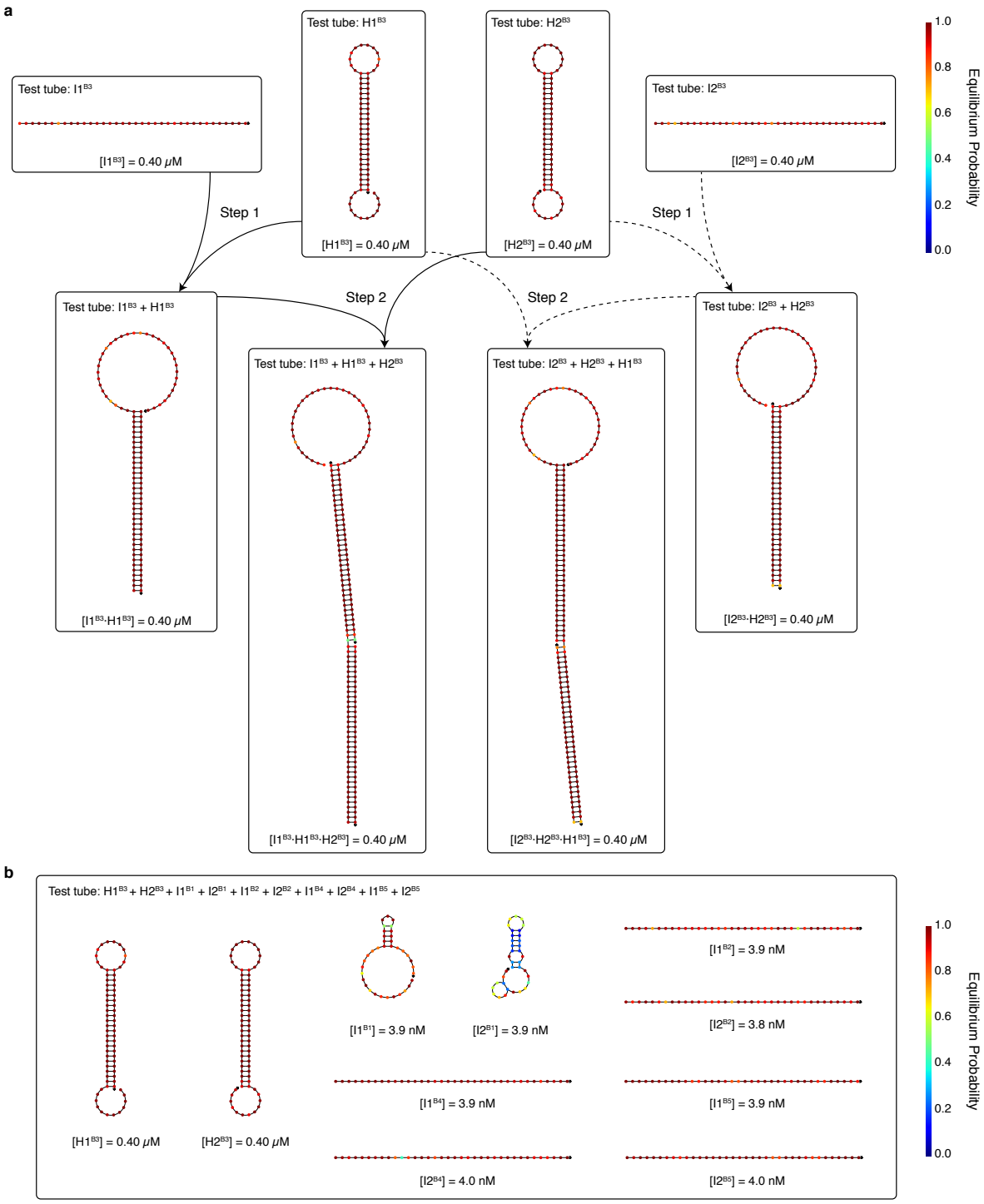

Figure S7. Computational analysis of DNA HCR amplifier B3. (a) Stepping study. Equilibrium test tube calculations predict that initiators, hairpins, and polymerization intermediates are well-formed with quantitative yield. (b) Orthogonality study. Equilibrium test tube calculations predict that polymerization is not triggered by the initiators for the other four amplifiers. (a,b) Each box represents a test tube containing the strands listed at the top at concentrations: 0.4 μM hairpins and initiators for panel a, 0.4 μM hairpins and 4 nM initiators for panel b. For each test tube, thermodynamic analysis yields the equilibrium concentrations and base-pairing ensemble properties for all complexes containing up to three strands. Each complex predicted to form with appreciable concentration at equilibrium is depicted by its minimum free energy structure, with each nucleotide shaded by the probability that it adopts the depicted base pairing state at equilibrium. The predicted equilibrium concentration is noted below each complex.

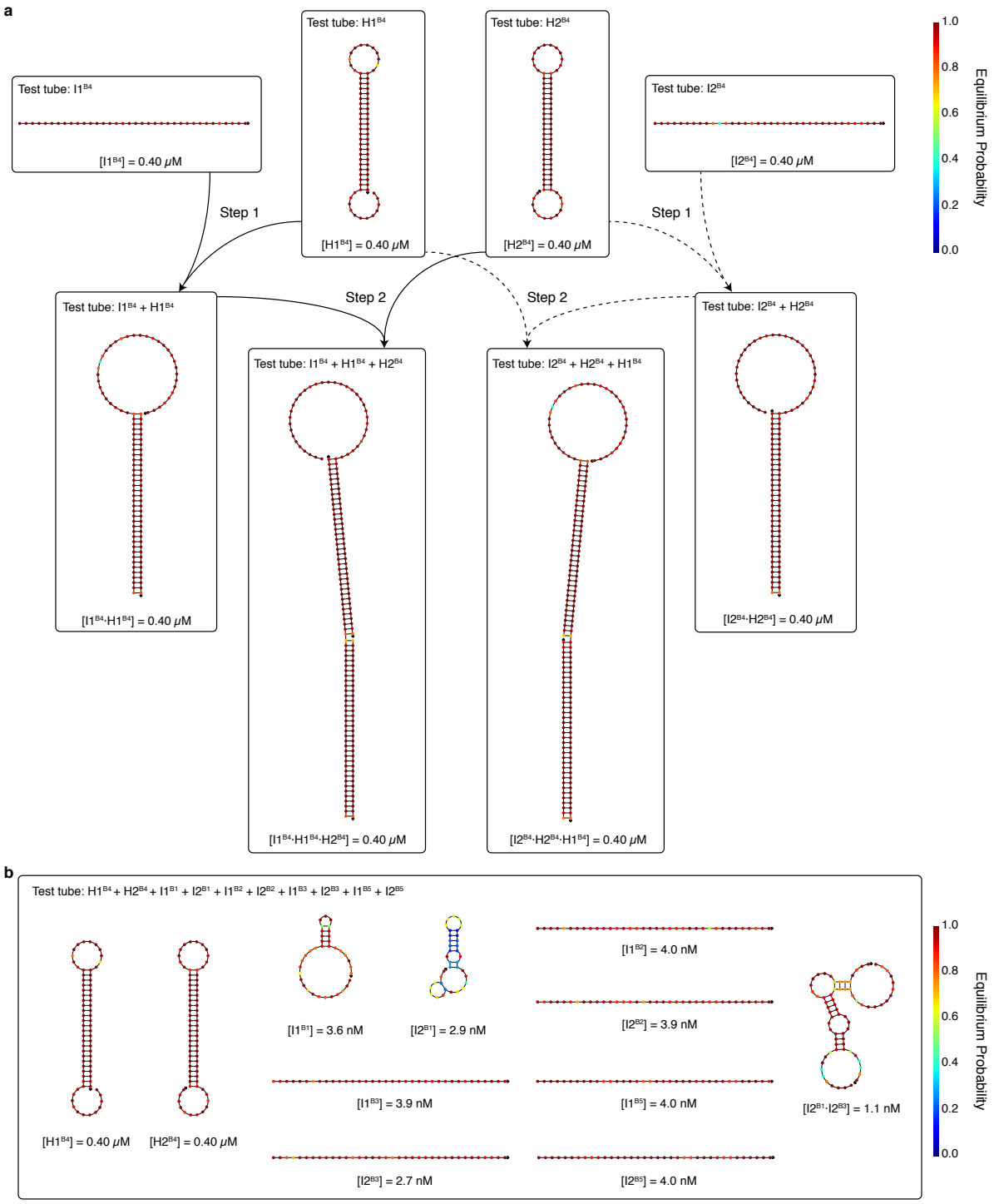

Figure S8. Computational analysis of DNA HCR amplifier B4. (a) Stepping study. Equilibrium test tube calculations predict that initiators, hairpins, and polymerization intermediates are well-formed with quantitative yield. (b) Orthogonality study. Equilibrium test tube calculations predict that polymerization is not triggered by the initiators for the other four amplifiers. (a,b) Each box represents a test tube containing the strands listed at the top at concentrations: 0.4 μM hairpins and initiators for panel a, 0.4 μM hairpins and 4 nM initiators for panel b. For each test tube, thermodynamic analysis yields the equilibrium concentrations and base-pairing ensemble properties for all complexes containing up to three strands. Each complex predicted to form with appreciable concentration at equilibrium is depicted by its minimum free energy structure, with each nucleotide shaded by the probability that it adopts the depicted base pairing state at equilibrium. The predicted equilibrium concentration is noted below each complex.

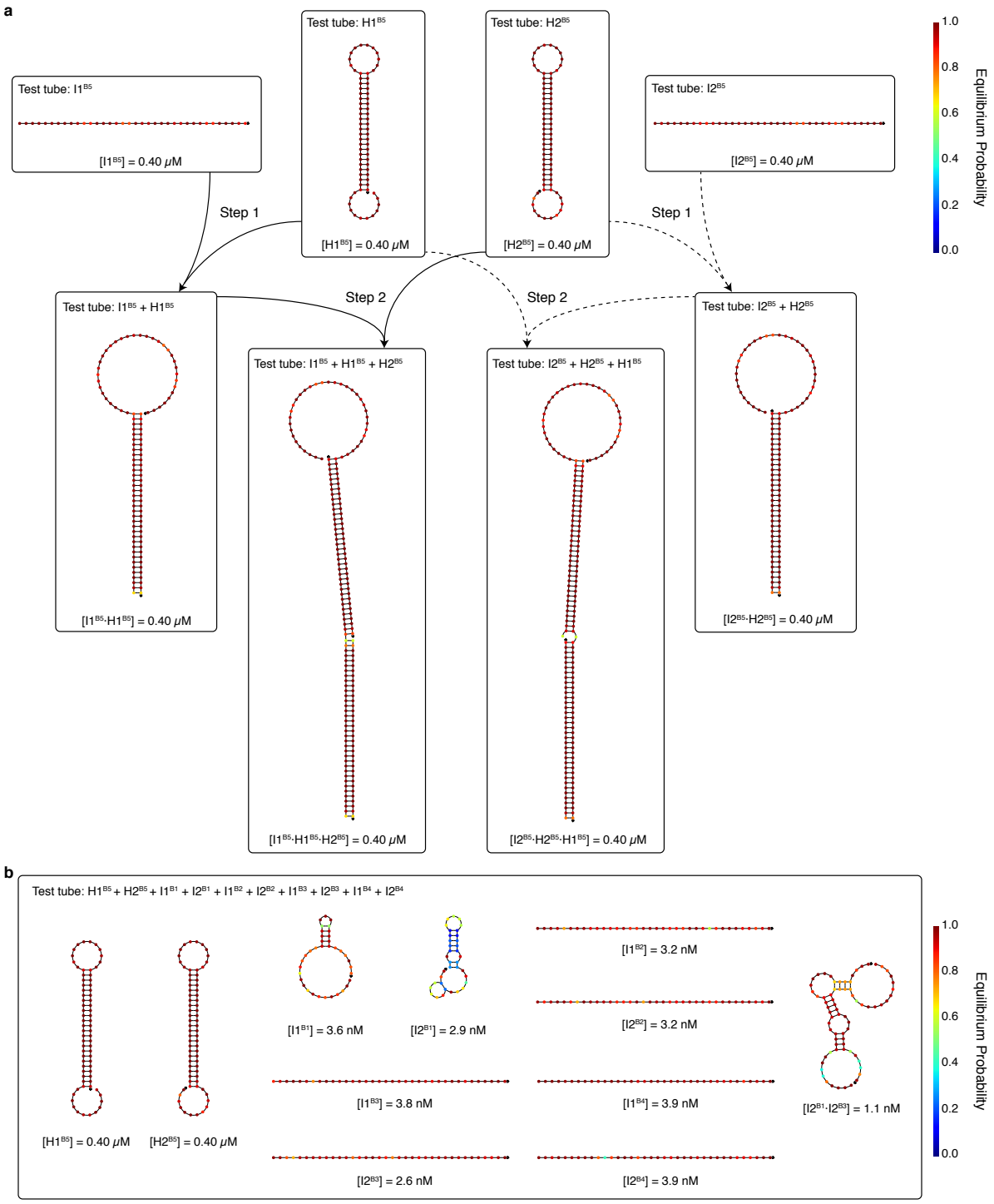

Figure S9. Computational analysis of DNA HCR amplifier B5. (a) Stepping study. Equilibrium test tube calculations predict that initiators, hairpins, and polymerization intermediates are well-formed with quantitative yield. (b) Orthogonality study. Equilibrium test tube calculations predict that polymerization is not triggered by the initiators for the other four amplifiers. (a,b) Each box represents a test tube containing the strands listed at the top at concentrations: 0.4 μM hairpins and initiators for panel a, 0.4 μM hairpins and 4 nM initiators for panel b. For each test tube, thermodynamic analysis yields the equilibrium concentrations and base-pairing ensemble properties for all complexes containing up to three strands. Each complex predicted to form with appreciable concentration at equilibrium is depicted by its minimum free energy structure, with each nucleotide shaded by the probability that it adopts the depicted base pairing state at equilibrium. The predicted equilibrium concentration is noted below each complex.

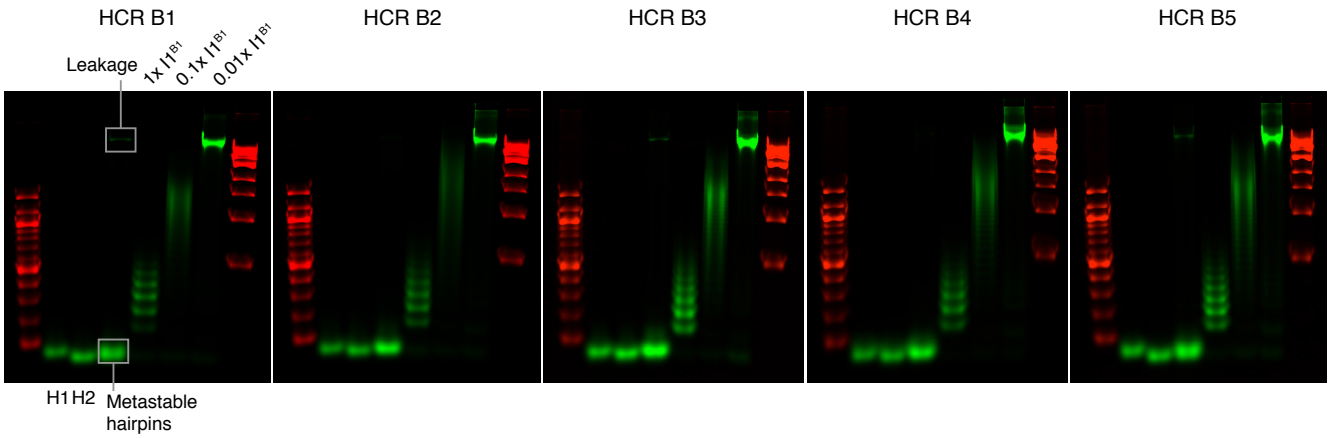

Figure S10. Experimental validation of conditional polymerization for five DNA HCR amplifiers (B1–B5). For each amplifier, the hairpins (H1 and H2) exhibit metastability in the absence of a cognate initiator and undergo conditional polymerization upon the introduction of a cognate initiator (I1). Mean polymer length increases with decreasing initiator concentration. Agarose gel electrophoresis using reaction conditions from Figure 2b (1 μM for each hairpin, $1\times$, $0.1\times$, $0.01\times$ for initiator I1, overnight reaction). Each gel tests the hairpins for one HCR amplifier. All hairpins were labeled with Alexa 647 (green channel). Native 1% agarose gels were run at 100 V for 100 min and imaged with a 635 nm laser and a 665 nm longpass filter. The 100 bp and 1 kb DNA ladders (red channel) were pre-stained with SYBR Gold and imaged using a 488 nm laser and a 575 nm long pass filter.

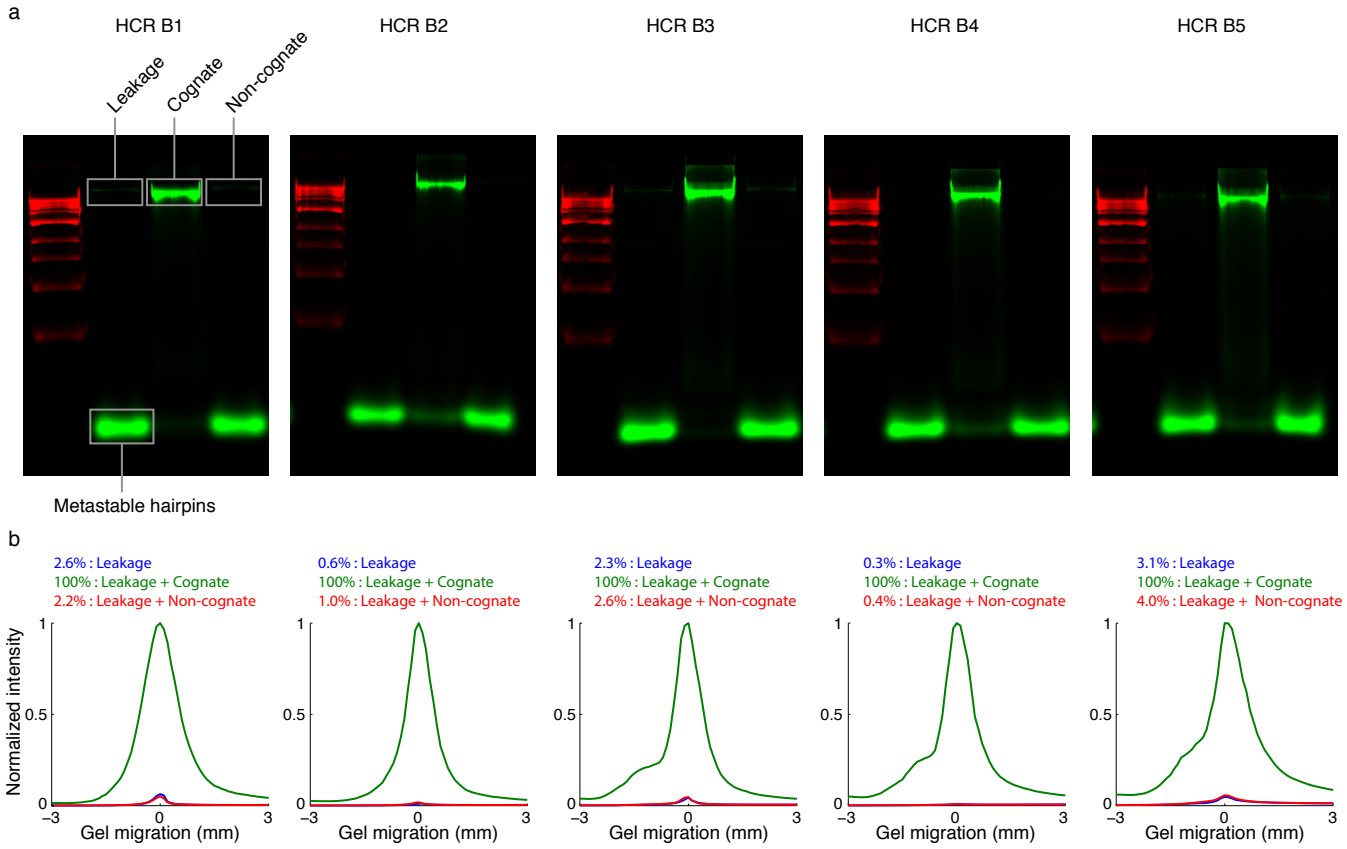

Figure S11. Experimental validation of orthogonality for five DNA HCR amplifiers (B1–B5). For each amplifier, the hairpins (H1 and H2) exhibit metastability in the absence of a cognate initiator (leakage lane), undergo conditional polymerization upon introduction of a cognate initiator (cognate lane), and do *not* polymerize upon introduction of the initiators for the other four amplifiers (non-cognate lane). (a) Agarose gel electrophoresis using reaction conditions from Figure 3 (400 nM for each hairpin, 4 h reaction). Each gel tests the hairpins for one HCR amplifier. Leakage: no initiator. Cognate: one cognate initiator (I1). Non-cognate: eight non-cognate initiators (I1 and I2 for each of four other HCR amplifiers). Each initiator at 4 nM (0.01× hairpin concentration). All hairpins were labeled with Alexa 647 (green channel). Native 1% agarose gels were run at 100 V for 100 min and imaged with a 635 nm laser and a 665 nm longpass filter. The 1 kb DNA ladder (red channel) was pre-stained with SYBR Gold and imaged using a 488 nm laser and a 575 nm long pass filter. (b) Quantification of the polymer bands in panel (a). Multi Gauge software (Fuji Photo Film) was used to calculate the Alexa 647 intensity profile surrounding the polymer band for three lanes in each gel (leakage, cognate, non-cognate). Each intensity profile is displayed for ± 3 mm of gel migration distance with the peak value centered at 0; the intensity values are normalized so that the highest peak value for each gel is set to 1. The quantification percentages were calculated using Multi Gauge with auto-detection of signal and background; the calculated values were normalized to the measured value for the cognate lane. Based on repeated analysis using Multi Gauge, the uncertainty in quantifying the bands in any given gel is estimated to be less than 0.1% of the cognate band signal used for normalization.

S4 Characterization of background and signal *in situ*

Fluorescent background (BACK) in each pixel is generated by three sources:

- **Autofluorescence (AF):** inherent fluorescence of the fixed sample.
- **Non-specific amplification (NSA):** HCR hairpins that bind non-specifically in the sample.
- **Non-specific detection (NSD):** probes that bind non-specifically in the sample and are subsequently amplified.

Hence, BACK = AF + NSA + NSD. Fluorescent signal (SIG) in each pixel is generated by HCR amplification polymers tethered to probes bound specifically to a target mRNA. The total fluorescence in a pixel is BACK + SIG.

For the *in situ* validation studies of Figures 4, 5, and 6, we use a transgenic target mRNA so that NSD can be characterized in a WT embryo lacking the target. The contributions of AF, NSA, NSD, and SIG to the total fluorescence are characterized using the following four types of experiments:

- **AF:** transgenic embryo (Target +), *in situ* protocol omitting probes and hairpins.
- **AF + NSA:** transgenic embryo (Target +), *in situ* protocol omitting probes.
- **AF + NSA + NSD:** WT embryo (Target -), standard *in situ* protocol.
- **AF + NSA + NSD + SIG:** transgenic embryo (Target +), standard *in situ* protocol.

For each of the *in situ* studies of Figures 4, 5, and 6, replicates (N=3 embryos) are shown for each of these four types of experiment in Sections S4.1, S4.2, and S4.3. For each embryo, we analyze pixels in a representative rectangular region of a representative optical section. For the pixels in a given rectangle, we characterize the distribution by plotting a pixel intensity histogram and characterize typical performance by calculating the mean pixel intensity. These values are used to estimate the mean and standard deviation across embryos for each type of experiment (mean and standard deviation over N=3 rectangles, one per embryo). These quantities are then used to estimate the mean and standard deviation for the individual background and signal contributions (AF, NSA, NSD, SIG) using uncertainty propagation following the approach described in Materials and Methods.[8]

For the four-channel *in situ* validation study of Figure 7 (which uses three endogenous target mRNAs and one transgenic target mRNA), we analyze each channel separately, and characterize background and signal for the pixels contained in two rectangles per image: BACK is characterized using a rectangle in a region of low- or non-expression and BACK + SIG is characterized using a rectangle in a region of high expression (Section S4.4).

S4.1 Additional data for RNA HCR vs DNA HCR studies of Figure 4

Background and signal contributions are summarized for RNA HCR and DNA HCR in Table S1 and Figure S12 for the replicates shown in Figures S13 and S14. These embryos were imaged with the microscope gain set to avoid saturating pixels in the DNA HCR images (row 4 of Figure S14). With this setting, it was difficult to identify regions of signal in the RNA HCR images, making it difficult to appropriately place rectangles for characterization of pixel intensities. To assist with rectangle placement, the embryos for the RNA HCR studies of Figure S13 were also imaged with a higher microscope gain (Figure S15). The resulting rectangle placements were then used for the images of Figure S13. RNA HCR and DNA HCR experiments were performed using the protocols of Sections S1.3 and S1.5.

	RNA HCR	DNA HCR
Autofluorescence (AF)	5.4 ± 0.2	12.4 ± 0.5
Non-specific amplification (NSA)	3.6 ± 0.6	9.8 ± 0.8
Non-specific detection (NSD)	2.9 ± 0.6	8.9 ± 0.8
Background (BACK=AF+NSA+NSD)	11.8 ± 0.2	31.0 ± 0.4
Signal (SIG)	260 ± 20	1340 ± 30

Table S1. Estimated signal and background fluorescence intensities in representative rectangles (mean $\pm$ standard deviation, N=3 embryos) using RNA HCR and DNA HCR *in situ* amplification. Images and rectangle placements are shown in Figures S13 and S14.

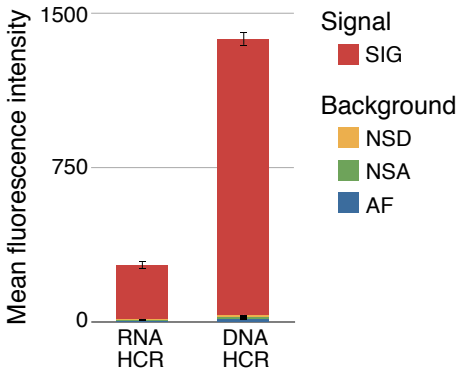

Figure S12. Signal and background contributions of Table S1.

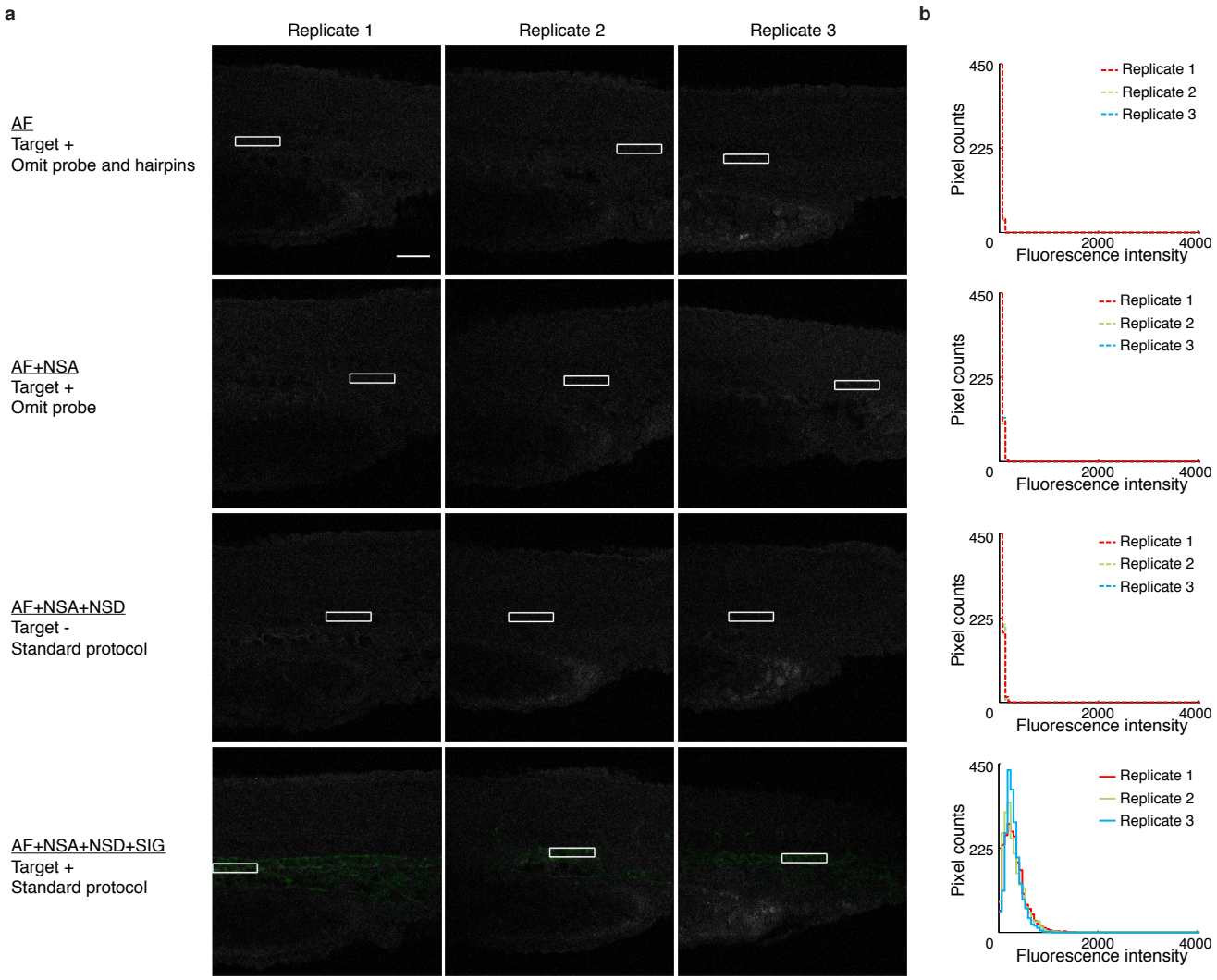

Figure S13. In situ amplification performance for published RNA HCR[1] in stringent amplification conditions. (a) Confocal images collected with the microscope PMT gain adjusted to avoid saturating pixels using DNA HCR (Figure S14, row 4). Target: transgenic mRNA *Tg(flk1:egfp)*. Probe set: a 1-initiator RNA probe. Samples: transgenic whole-mount zebrafish embryos containing the target (Target +) or WT embryos lacking the target (Target -). Green channel (excitation 633 nm): HCR-Alexa647 staining plus autofluorescence. Gray channel (excitation 488 nm): autofluorescence to depict sample morphology. (b) Pixel intensity histograms for one rectangle per sample. Embryos fixed: 27 hpf. Scale bar: 50 μm.

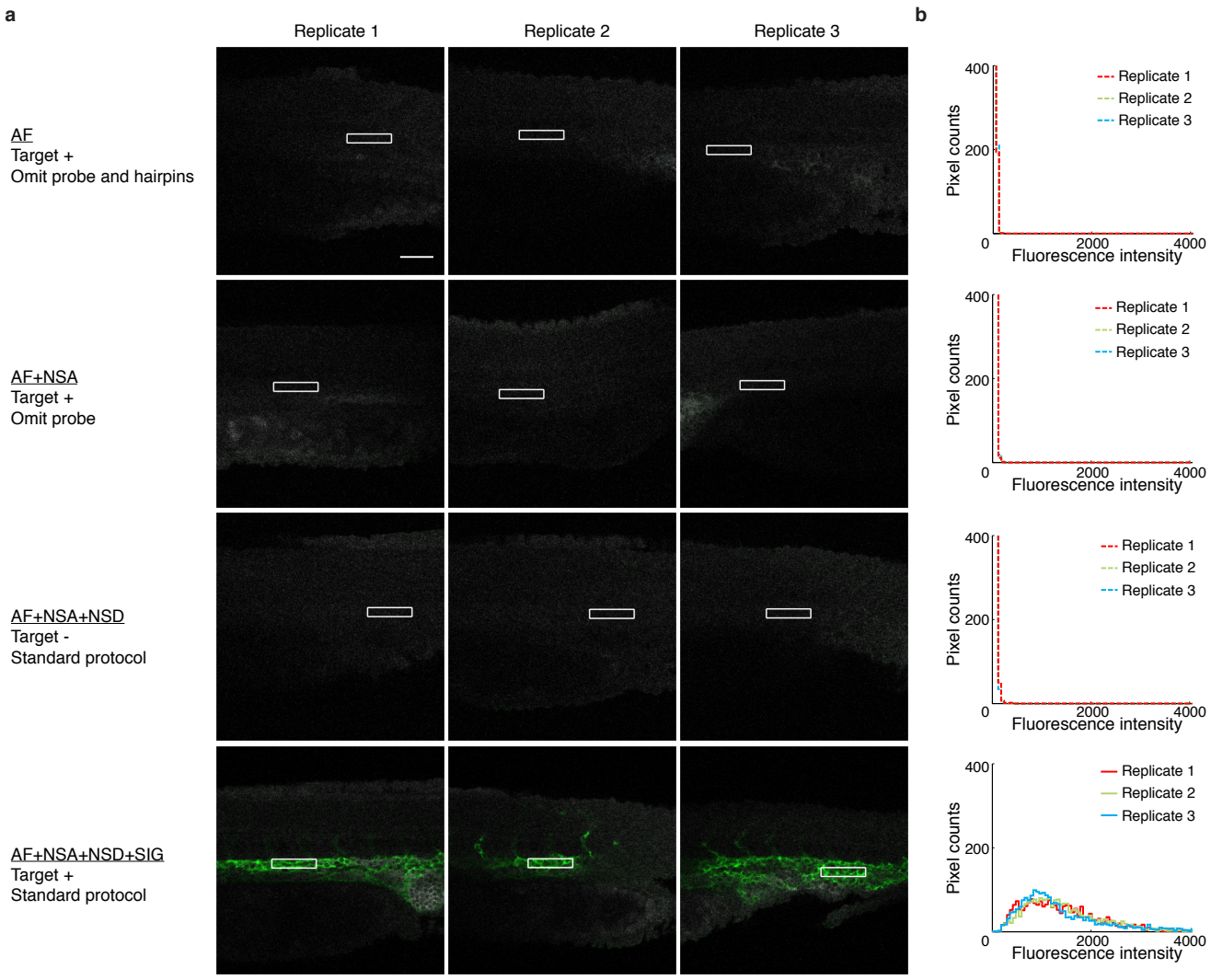

Figure S14. In situ amplification performance for next-generation DNA HCR in permissive amplification conditions. (a) Confocal images collected with the microscope PMT gain adjusted to avoid saturating pixels using DNA HCR (row 4). Target: transgenic mRNA *Tg(flk1:egfp)*. Probe set: a 1-initiator DNA probe. Samples: transgenic whole-mount zebrafish embryos containing the target (Target +) or WT embryos lacking the target (Target -). Green channel (excitation 633 nm): HCR-Alexa647 staining plus autofluorescence. Gray channel (excitation 488 nm): autofluorescence to depict sample morphology. (b) Pixel intensity histograms for one rectangle per sample. Embryos fixed: 27 hpf. Scale bar: 50 μm.

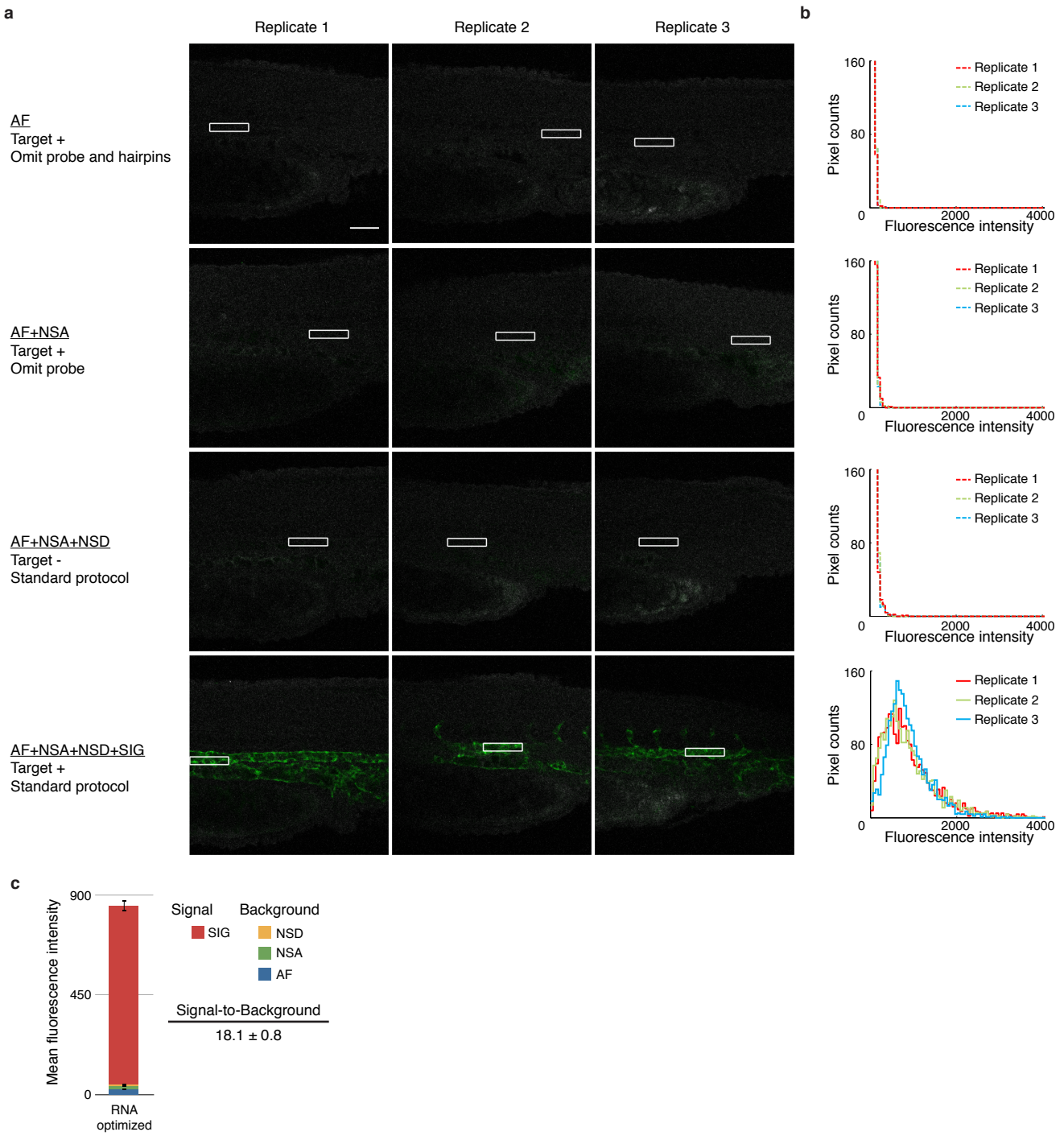

Figure S15. In situ amplification performance for published RNA HCR[1] in stringent amplification conditions with the microscope PMT gain increased. (a) The embryos from Figure S13 were re-imaged with the microscope PMT gain optimized for RNA HCR. Target: transgenic mRNA *Tg(flk1:egfp)*. Probe set: a 1-initiator RNA probe. Samples: transgenic whole-mount zebrafish embryos containing the target (Target +) or WT embryos lacking the target (Target -). Green channel (excitation 633 nm): HCR-Alexa647 staining plus autofluorescence. Gray channel (excitation 488 nm): autofluorescence to depict sample morphology. (b) Pixel intensity histograms for one rectangle per sample. (c) Estimated signal and background fluorescence intensities in representative rectangles (mean ± standard deviation, N=3 embryos). AF = 23.1 ± 0.6, NSA = 15 ± 1, NSD = 7 ± 2, BACK = 45 ± 2, SIG = 810 ± 20. Embryos fixed: 27 hpf. Scale bar: 50 μm.

S4.2 Additional data for direct-labeled probe studies of Figure 5

Background and signal contributions are summarized for direct-labeled DNA probes without and with DNA HCR *in situ* amplification in Table S2 and Figure S16 for the replicates shown in Figure S17. These embryos were imaged with the microscope gain set to avoid saturating pixels in the DNA HCR images (row 6 of Figure S17). With this setting, it was difficult to identify regions of signal for unamplified experiments, making it difficult to appropriately place rectangles for characterization of pixel intensities. To assist with rectangle placement, the embryos for the unamplified experiments were also imaged with a higher microscope gain (Figure S18). The resulting rectangle placements were then used for the images in the first three rows of Figure S17. Experiments were performed using the protocol of Section S1.5.

	Probe	HCR
Autofluorescence (AF)	0.5 ± 0.1	0.5 ± 0.1
Non-specific amplification (NSA)	—	0.3 ± 0.1
Non-specific detection (NSD)	0.3 ± 0.1	28.0 ± 0.4
Background (BACK = AF+NSA+NSD)	0.8 ± 0.1	28.7 ± 0.4
Signal (SIG)	9 ± 1	2010 ± 70

Table S2. Estimated signal and background fluorescence intensities in representative rectangles (mean $\pm$ standard deviation, N=3 embryos) using direct-labeled DNA probes without and with DNA HCR *in situ* amplification. Images and rectangle placements are shown in Figure S17.

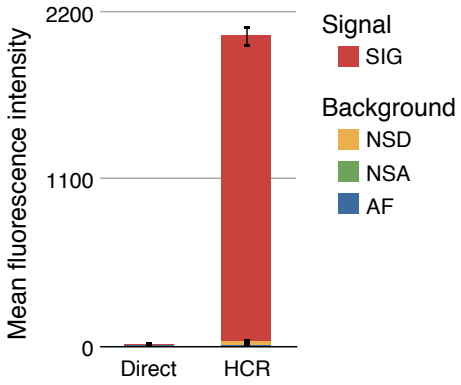

Figure S16. Signal and background contributions of Table S2.

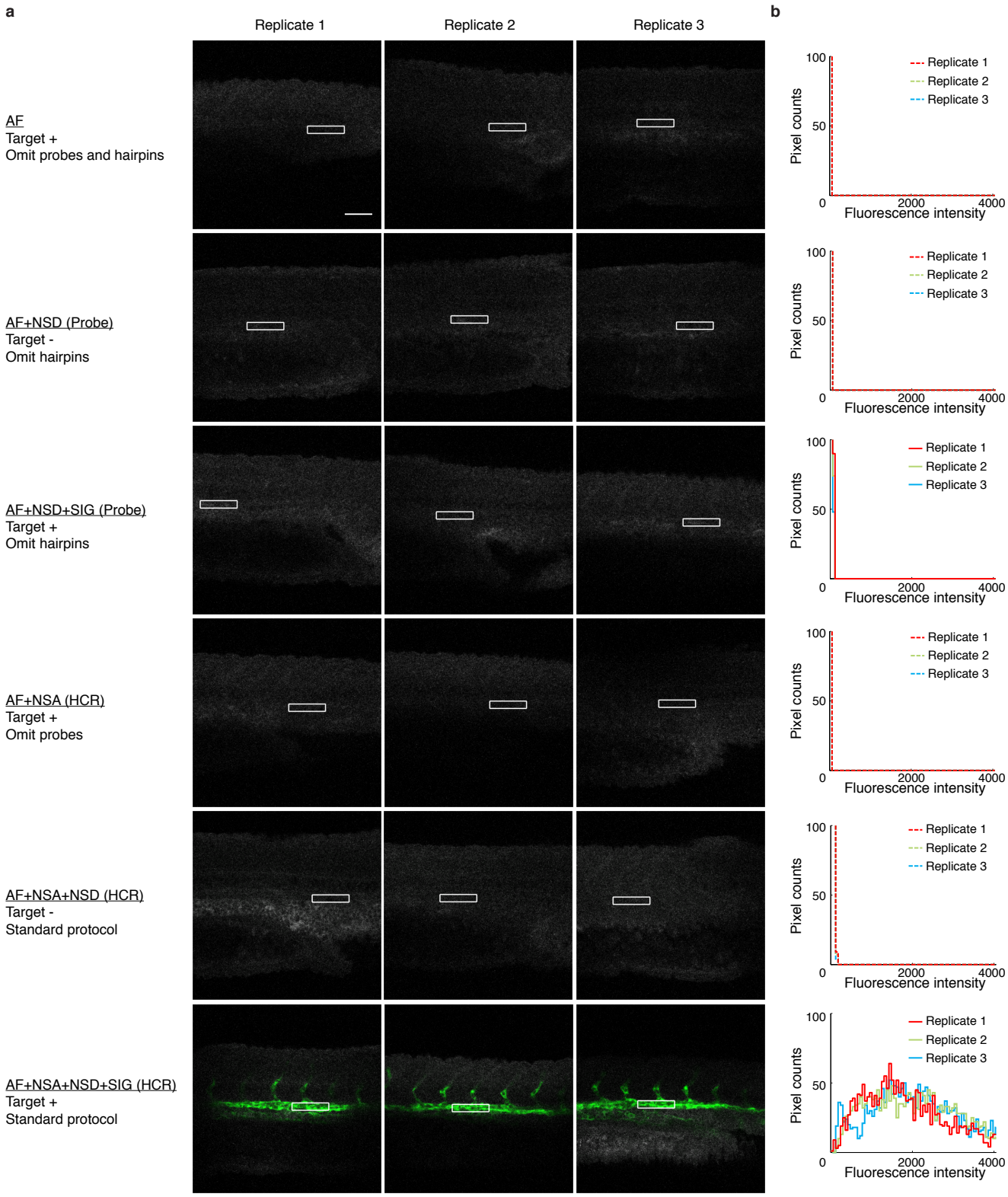

Figure S17. Comparing signal strength using direct-labeled DNA probes without and with DNA HCR *in situ* amplification. (a) Confocal images collected with the microscope PMT gain adjusted to avoid saturating pixels using DNA HCR (row 6). Target: transgenic mRNA *Tg(flk1:egfp)*. Probe set: five Alexa647-labeled 1-initiator DNA probes. Samples: transgenic whole-mount zebrafish embryos containing the target (Target +) or WT embryos lacking the target (Target -). Green channel (excitation 633 nm): probe-Alexa647 and/or HCR-Alexa647 staining plus autofluorescence. Gray channel (excitation 488 nm): autofluorescence to depict sample morphology. (b) Pixel intensity histograms for one rectangle per sample. Embryos fixed: 27 hpf. Scale bar: 50 μm.

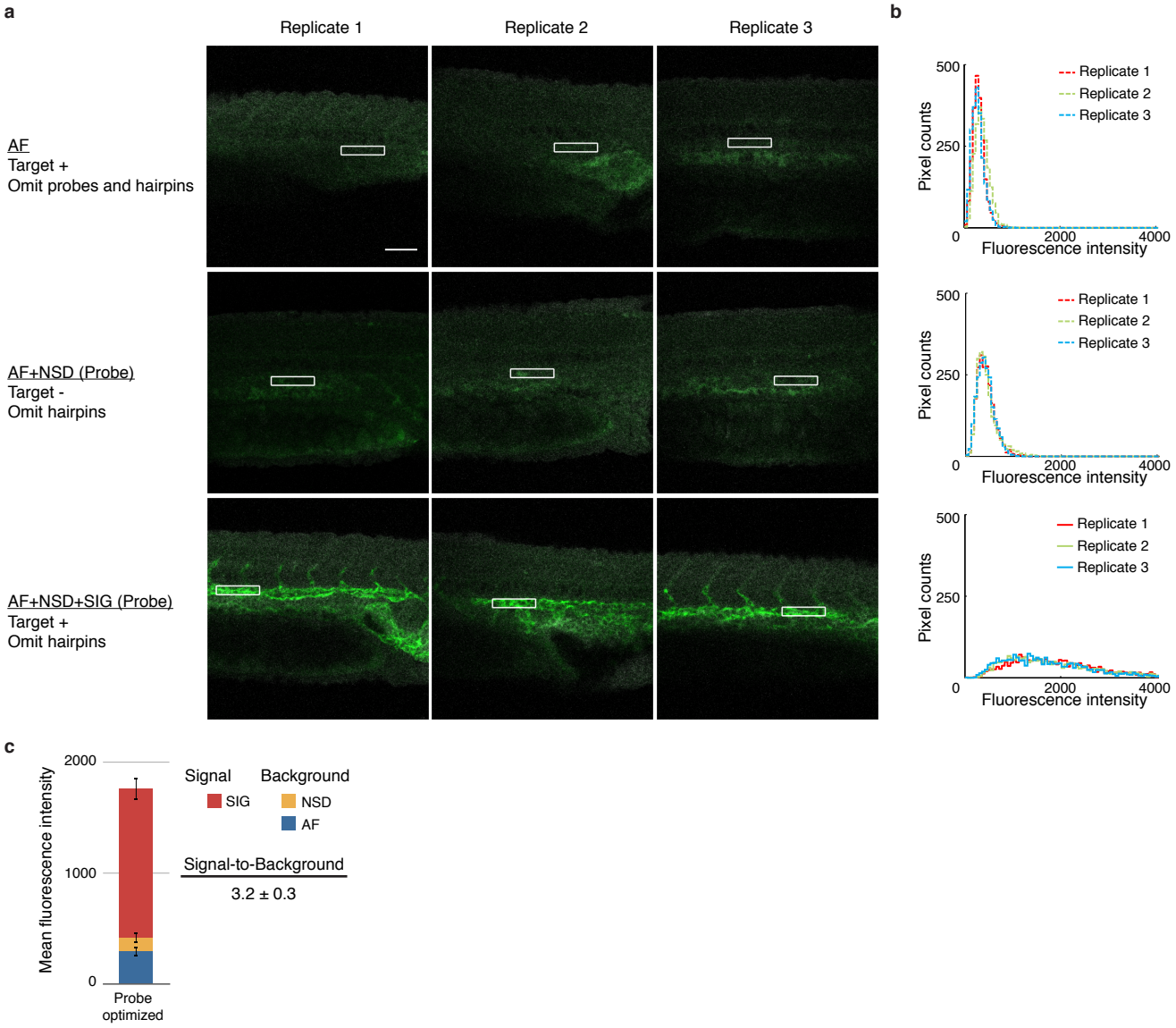

Figure S18. Signal strength using direct-labeled DNA probes with the microscope PMT gain increased. (a) The embryos from Figure S17 (rows 1–3) were re-imaged with the microscope PMT gain optimized for direct-labeled probes. Target: transgenic mRNA *Tg(flk1:egfp)*. Probe set: five Alexa647-labeled 1-initiator DNA probes. Samples: transgenic whole-mount zebrafish embryos containing the target (Target +) or WT embryos lacking the target (Target -). Green channel (excitation 633 nm): probe-Alexa647 staining plus autofluorescence. Gray channel (excitation 488 nm): autofluorescence to depict sample morphology. (b) Pixel intensity histograms for one rectangle per sample. (c) Estimated signal and background fluorescence intensities in representative rectangles (mean ± standard deviation, N=3 embryos). AF = 290 ± 50, NSD = 130 ± 50, BACK = 420 ± 20, SIG = 1300 ± 100. Embryos fixed: 27 hpf. Scale bar: 50 μm.

S4.3 Additional data for 1-initiator vs 2-initiator studies of Figure 6

Background and signal contributions are summarized for 1-initiator and 2-initiator DNA probe studies in Table S3 and Figure S19 for the replicates shown in Figures S20–S22. These embryos were imaged with the microscope gain set to avoid saturating pixels in the 2-initiator images (row 4 of Fig. S22). Experiments were performed using the protocol of Section S1.5.

	1-initiator (I1)	1-initiator (I2)	2-initiator (I1+I2)
Autofluorescence (AF)	3.9 ± 0.2	3.9 ± 0.2	3.9 ± 0.2
Non-specific amplification (NSA)	3.4 ± 0.3	3.4 ± 0.3	3.4 ± 0.3
Non-specific detection (NSD)	4 ± 2	9.4 ± 0.4	11 ± 1
Background (BACK=AF+NSA+NSD)	12 ± 2	16.6 ± 0.4	19 ± 1
Signal (SIG)	640 ± 40	930 ± 40	1590 ± 50

Table S3. Estimated signal and background fluorescence intensities in representative rectangles (mean $\pm$ standard deviation, N=3 embryos) using DNA HCR amplification with 1-initiator or 2-initiator DNA probes. Images and rectangle placements are shown in Figures S20–S22.

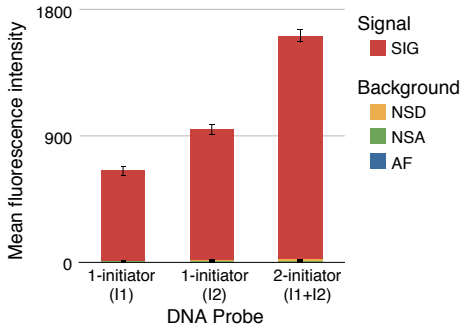

Figure S19. Signal and background contributions of Table S3.

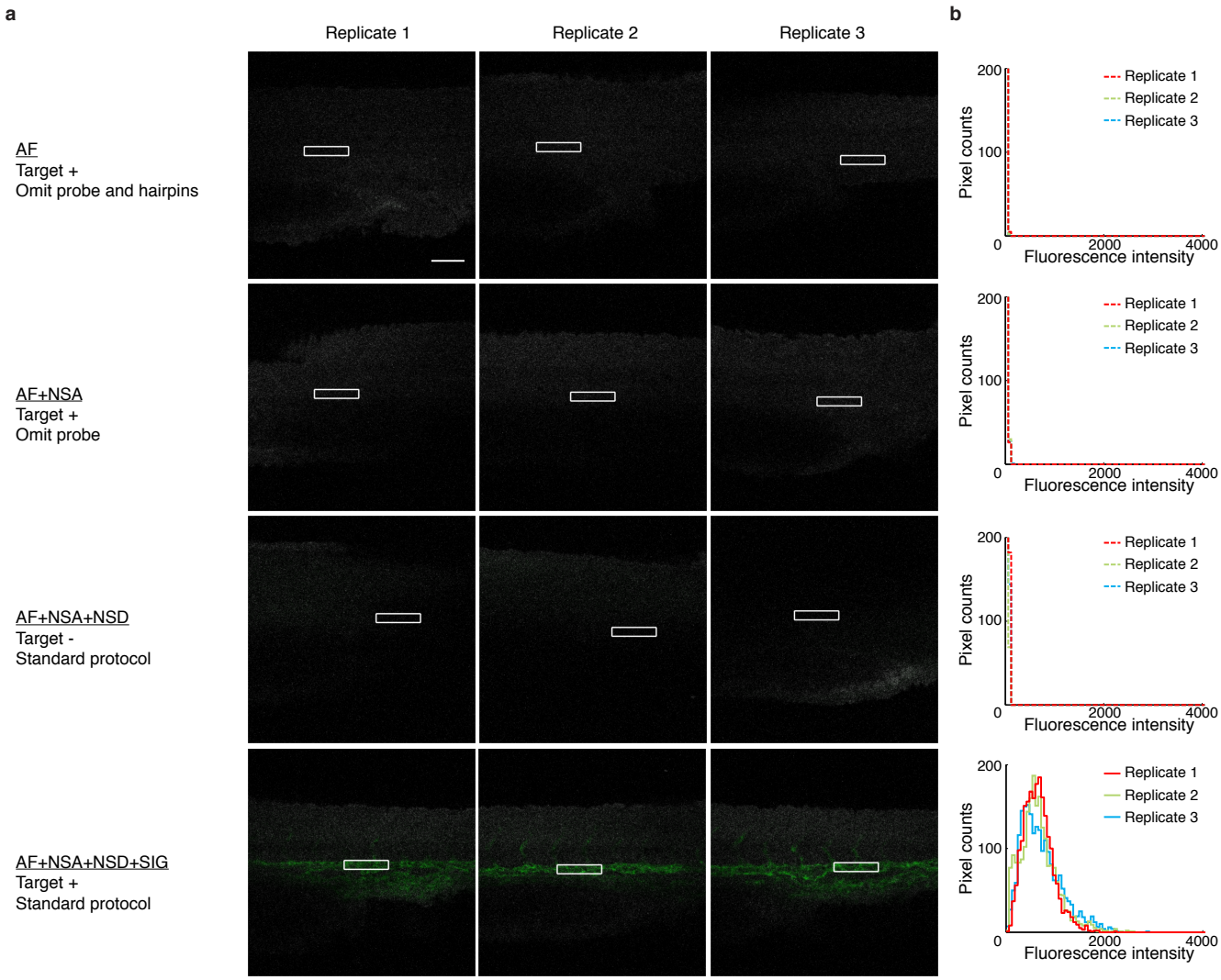

Figure S20. Signal strength using DNA HCR *in situ* amplification with a 1-initiator DNA probe (initiator I1). (a) Confocal images collected with the microscope gain adjusted to avoid saturating pixels using the 2-initiator DNA probe (Fig. S22, row 4). Target: transgenic mRNA *Tg(flk1:egfp)*. Probe set: a 1-initiator DNA probe (I1). Samples: transgenic whole-mount zebrafish embryos containing the target (Target +) or WT embryos lacking the target (Target -). Green channel (excitation 633 nm): HCR-Alexa647 staining plus autofluorescence. Gray channel (excitation 488 nm): autofluorescence to depict sample morphology. (b) Pixel intensity histograms for one rectangle per sample. Embryos fixed: 27 hpf. Scale bar: 50 μm.

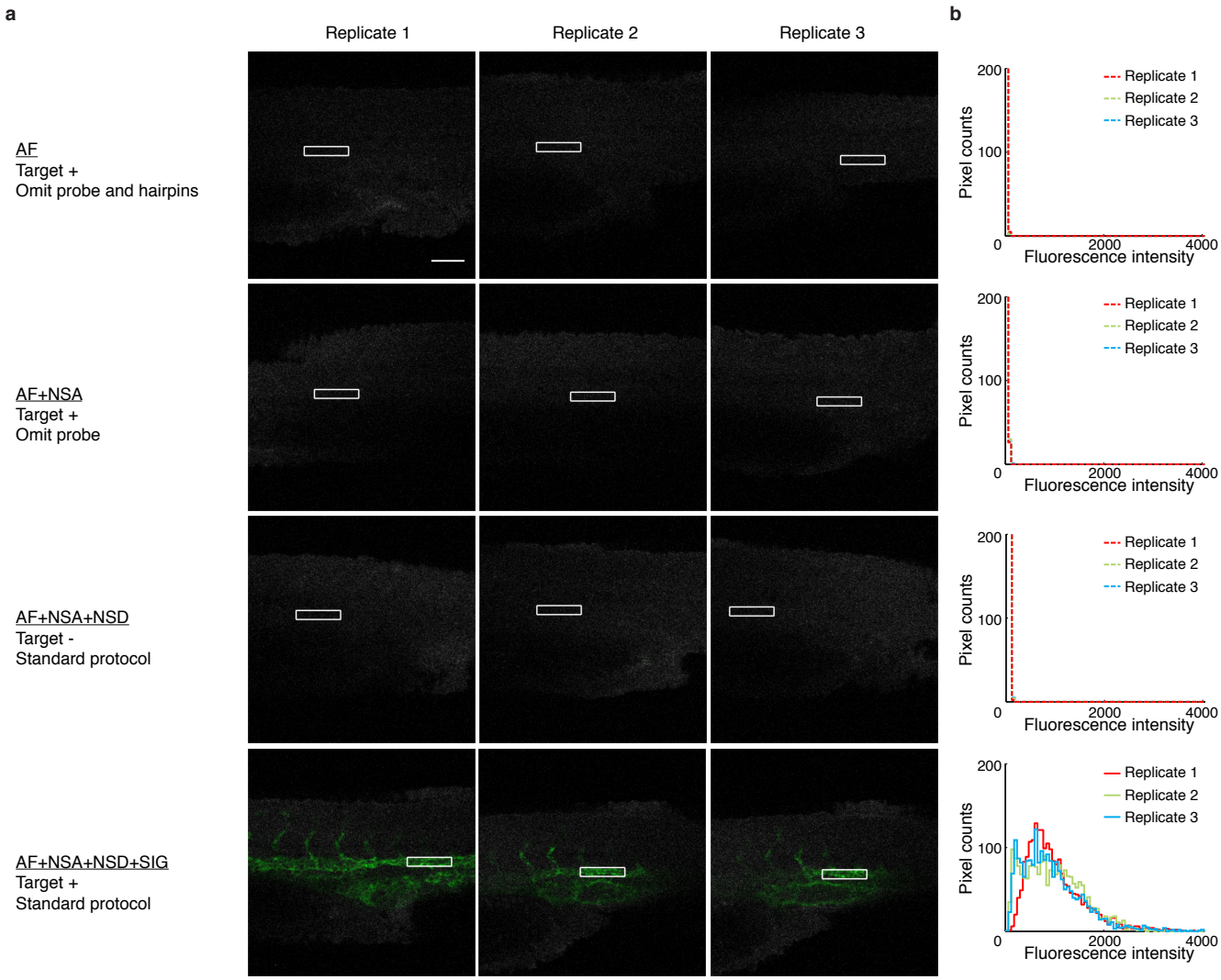

Figure S21. Signal strength using DNA HCR *in situ* amplification with a 1-initiator DNA probe (initiator I2). (a) Confocal images collected with the microscope gain adjusted to avoid saturating pixels using the 2-initiator DNA probe (Fig. S22, row 4). Target: transgenic mRNA *Tg(flk1:egfp)*. Probe set: a 1-initiator DNA probe (I2). Samples: transgenic whole-mount zebrafish embryos containing the target (Target +) or WT embryos lacking the target (Target -). Green channel (excitation 633 nm): HCR-Alexa647 staining plus autofluorescence. Gray channel (excitation 488 nm): autofluorescence to depict sample morphology. (b) Pixel intensity histograms for one rectangle per sample. Embryos fixed: 27 hpf. Scale bar: 50 μm.

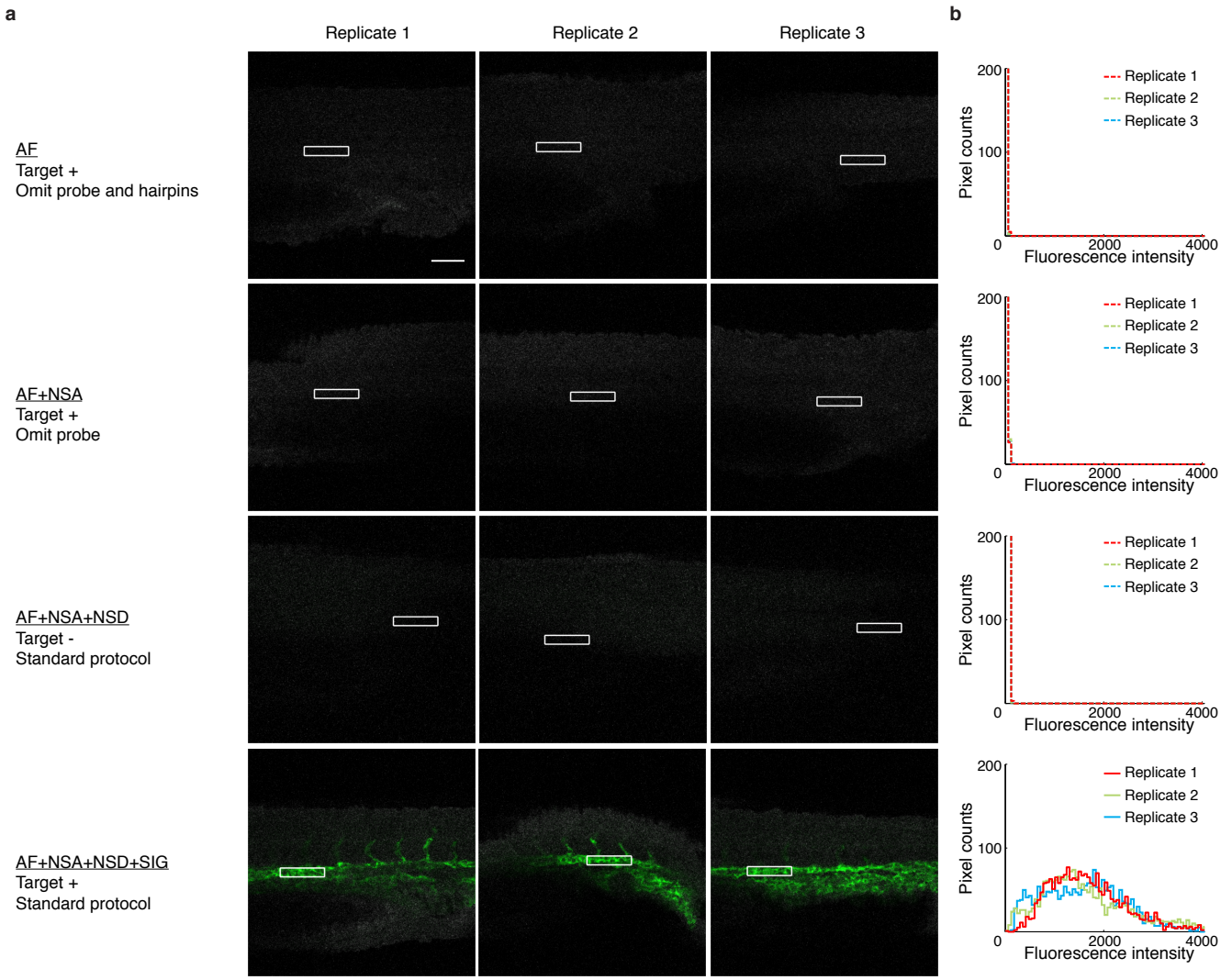

Figure S22. Signal strength using DNA HCR *in situ* amplification with a 2-initiator DNA probe (initiators I1 and I2). (a) Confocal images collected with the microscope gain adjusted to avoid saturating pixels using the 2-initiator DNA probe (row 4). Target: transgenic mRNA *Tg(flk1:egfp)*. Probe set: a 2-initiator DNA probe (I1 + I2). Samples: transgenic whole-mount zebrafish embryos containing the target (Target +) or WT embryos lacking the target (Target -). Green channel (excitation 633 nm): HCR-Alexa647 staining plus autofluorescence. Gray channel (excitation 488 nm): autofluorescence to depict sample morphology. (b) Pixel intensity histograms for one rectangle per sample. Embryos fixed: 27 hpf. Scale bar: 50 μm.

S4.4 Additional data for multiplexed studies of Figure 7

Signal-to-background ratios are shown for four target mRNAs in Table S4 based on the replicates in Figure S23. Experiments were performed using the protocol of Section S1.5.

	Tg(flk1:egfp)	*tpm3*	*elavl3*	*ntla*
Background	32.8 ± 0.5	46 ± 6	60 ± 20	52 ± 8
Signal	1800 ± 200	1100 ± 200	670 ± 60	930 ± 60
Signal-to-background	54 ± 7	25 ± 5	11 ± 3	18 ± 3

Table S4. Estimated signal-to-background (mean $\pm$ standard deviation, N=3 embryos) for four target mRNAs based on images and rectangles of Figure S23.

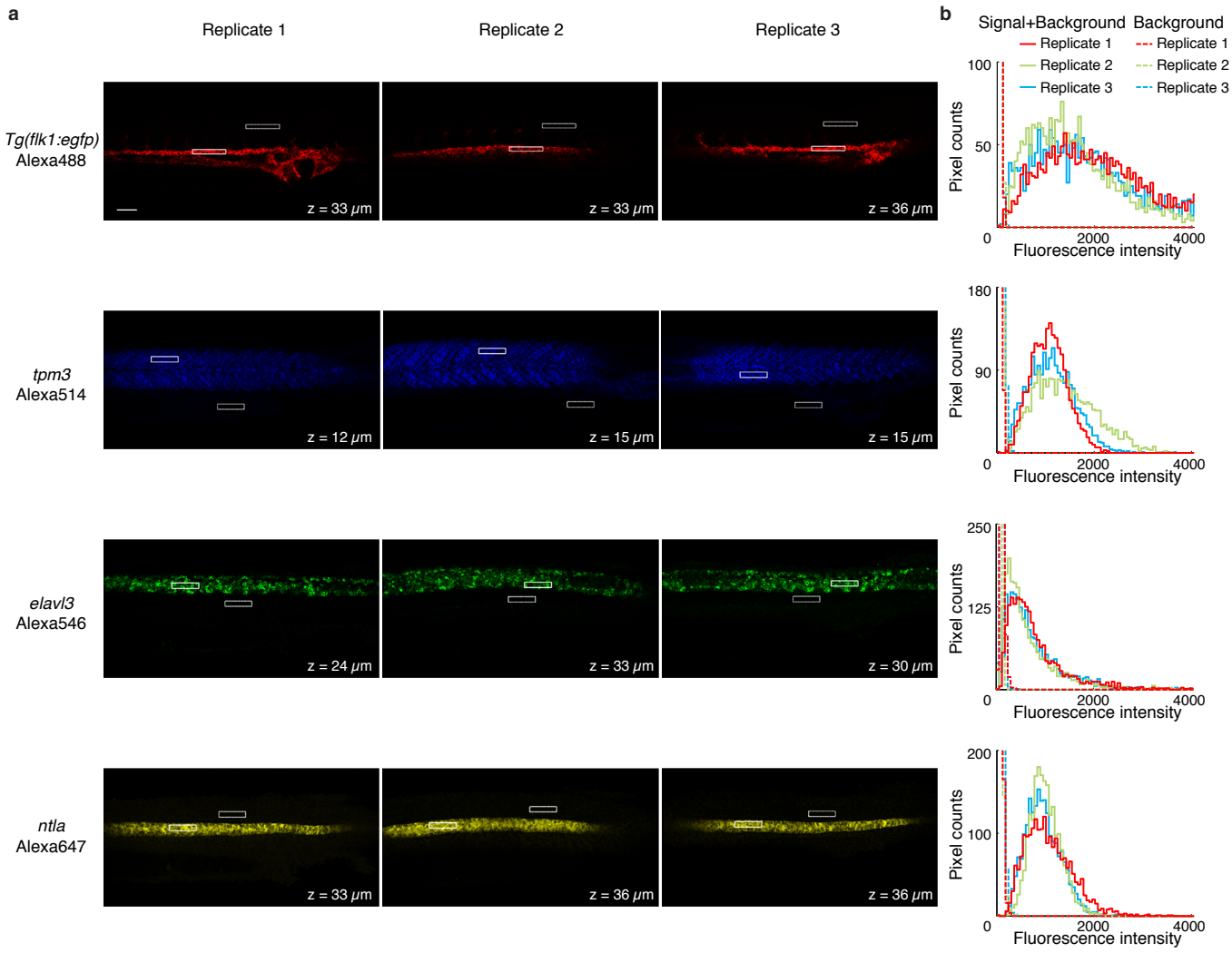

Figure S23. Multiplexed *in situ* amplification performance using DNA HCR in fixed whole-mount zebrafish embryos. (a) Confocal images for four target mRNAs collected in four spectrally distinct fluorescence channels. For each of three embryos, a representative optical section is selected for each channel based on the expression depth of the corresponding target mRNA. (b) Pixel intensity histograms for one rectangle per image per channel (background + signal (solid line), background (dashed line)). Note that for speckled expression patterns (*e.g., elavl3*), there are a substantial number of non-expression pixels even in a rectangle placed in a region of high expression. These non-expression pixels pollute the 'background + signal' distribution with some 'background' pixels and artificially deflate the estimated signal-to-background ratio. However, even this underestimate of signal-to-background is an order of magnitude or more for each target mRNA. Embryos fixed: 27 hpf. Scale bar: 50 μm.

S4.5 Additional data for colocalization studies of Figure 8

We use the Pearson correlation coefficient, $r \in [-1, 1]$, to quantify the correlation between pixel intensities[9] for channels 1 and 2 of Figures 8a and S24a. To avoid inflating the correlation coefficient, we exclude pixels that fall below background thresholds in *both* channels (excluded pixels fall in the black box at the lower left corner of the correlation plot). For each channel, the background threshold is defined as the mean plus two standard deviations for the pixels in the depicted white square.

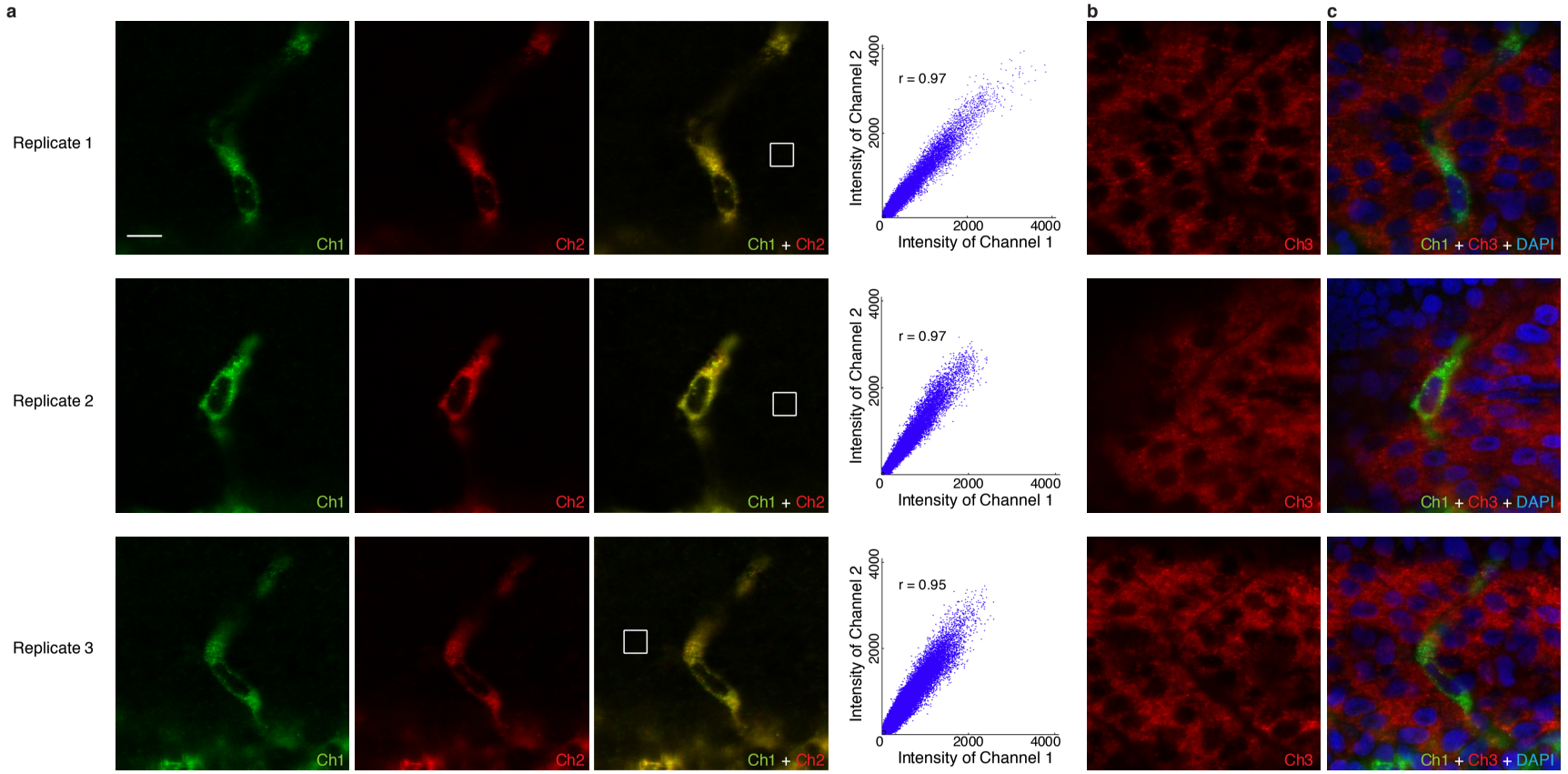

Figure S24. Redundant two-color mapping of a target mRNA expressed predominantly in the interstices between somites (*Tg(flk1:egfp)*; two probe sets, two amplifiers, channels 1 and 2) simultaneous with mapping of a target mRNA expressed predominantly in the somites (*desm*; channel 3) and nuclear staining with DAPI (channel 4). Confocal images collected with the microscope gain adjusted to avoid saturating pixels in each channel. (a) Colocalization of *Tg(flk1:egfp)* signal (each pixel is 129 nm $\times$ 129 nm); scatter plot and Pearson correlation coefficient for pixel intensities. (b) *desm* signal. (c) *Tg(flk1:egfp)* and *desm* signal with DAPI nuclear staining. Probe sets: three and five 2-initiator DNA probes for *Tg(flk1:egfp)*, three 2-initiator DNA probes for *desm*. Amplifiers: three orthogonal DNA HCR amplifiers carrying spectrally distinct fluorophores. Embryos fixed: 27 hpf. Scale bar: 10 μm.

S5 Probe sequences

Sequences for the five target mRNAs used in this paper were obtained from the Zebrafish Information Network (ZFIN).[10] All sequences are listed $5'$ to $3'$.

S5.1 Probe for Figure S3

A single 1-initiator DNA probe was used to detect the *egfp* target mRNA and initiate polymerization of DNA HCR amplifier B4.

Target mRNA: **enhanced green fluorescent protein (*egfp*)**
Amplifier: **DNA HCR B4**
Fluorophore: **Alexa Fluor 647**

Initiator I1	Spacer	Probe Sequence
CCTCAACCTACCTCCAACTCTCACCATATTCgCTTC	TAAAA	gTTCTTCTgCTTgTCggCCATgATATAgACgTTgTggCTgTTgTAgTTgT

S5.2 Probes for Figures 4, 6, S13–S15, and S20–S22

The *egfp* target mRNA was detected by a single probe. For RNA HCR studies, a single 1-initiator RNA probe was used to initiate RNA HCR amplifier A3 (Figs 4, S13, and S15). For DNA HCR studies, a single 1-initiator DNA probe with initiator I1 (Figs 4, 6, S14, S20) or initiator I2 (Figs 6 and S21) or a single 2-initiator DNA probe with initiators I1 and I2 (Figs 6 and S22) were used to initiate DNA HCR amplifier B1.

Target mRNA: **enhanced green fluorescent protein (*egfp*)**
Amplifier: **RNA HCR A3**
Fluorophore: **Alexa Fluor 647**

Initiator I1	Spacer	Probe Sequence
gACUACUgAUAACUggAUUgCCUUAg	AAUUU	gUUCUUCUgCUUgUCggCCAUgAUAUAgACgUUgUggCUgUUgUAgUUgU

Target mRNA: **enhanced green fluorescent protein (*egfp*)**
Amplifier: **DNA HCR B1**
Fluorophore: **Alexa Fluor 647**

Initiator I1	Spacer	Probe Sequence
gAggAgggCAgCAAACgggAAgAgTCTTCCTTTACg	ATATT	gTTCTTCTgCTTgTCggCCATgATATAgACgTTgTggCTgTTgTAgTTgT

Target mRNA: **enhanced green fluorescent protein (*egfp*)**
Amplifier: **DNA HCR B1**
Fluorophore: **Alexa Fluor 647**

Probe Sequence	Spacer	Initiator I2
gTTCTTCTgCTTgTCggCCATgATATAgACgTTgTggCTgTTgTAgTTgT	ATATA	gCATTCTTTCTTgAggAgggCAgCAAACgggAAgAg

Target mRNA: **enhanced green fluorescent protein (*egfp*)**
Amplifier: **DNA HCR B1**
Fluorophore: **Alexa Fluor 647**

Initiator I1	Spacer	Probe Sequence	Spacer	Initiator I2
gAggAgggCAgCAAACgggAAgAgTCTTCCTTTACg	ATATT	gTTCTTCTgCTTgTCggCCATgATATAgACgTTgTggCTgTTgTAgTTgT	ATATA	gCATTCTTTCTTgAggAgggCAgCAAACgggAAgAg

S5.3 Probes for Figures 5 and S17–S18

The probe set contains five direct-labeled probes, each carrying a single initiator for DNA HCR amplifier B1. For these studies, each probe and hairpin was labeled with a single Alexa Fluor 647.

`/5′-dye-C12/:` 5′ Alexa Fluor 647 modification with a C12 spacer

Target mRNA: **enhanced green fluorescent protein (*egfp*)**
Amplifier: **DNA HCR B1**
Fluorophore: **Alexa Fluor 647**

Initiator I1	Spacer	Probe Sequence
/5′-dye-C12/ gAggAgggCAgCAAACgggAAgAgTCTTCCTTTACg	ATATT	gTTCTTCTgCTTgTCggCCATgATATAgACgTTgTggCTgTTgTAgTTgT
/5′-dye-C12/ gAggAgggCAgCAAACgggAAgAgTCTTCCTTTACg	ATATT	TTCAgCTCgATgCggTTCACCAgggTgTCgCCCTCgAACTTCACCTCggC
/5′-dye-C12/ gAggAgggCAgCAAACgggAAgAgTCTTCCTTTACg	ATATT	ACgCTgCCgTCCTCgATgTTgTggCggATCTTgAAgTTCACCTTgATgCC
/5′-dye-C12/ gAggAgggCAgCAAACgggAAgAgTCTTCCTTTACg	ATATT	gCgggTCTTgTAgTTgCCgTCgTCCTTgAAgAAgATggTgCgCTCCTggA
/5′-dye-C12/ gAggAgggCAgCAAACgggAAgAgTCTTCCTTTACg	ATATT	CgTAgCCTTCgggCATggCggACTTgAAgAAgTCgTgCTgCTTCATgTgg

S5.4 Probes for Figures 7 and S23

Each of four target mRNAs is detected with a different probe set. Each probe set contains five 2-initiator DNA probes. Within a given probe set, each probe initiates the same DNA HCR amplifier.

Target mRNA: **enhanced green fluorescent protein (*egfp*)**
Amplifier: **DNA HCR B2**
Fluorophore: **Alexa Fluor 488**

Initiator I1	Spacer	Probe Sequence	Spacer	Initiator I2
CCTCgTAAATCCTCATCAATCATCCAgTAAACCgCC	AAAAA	gTTCTTCTgCTTgTCggCCATgATATAgACgTTgTggCTgTTgTAgTTgT	AAAAA	AgCTCAgTCCATCCTCgTAAATCCTCATCAATCATC
CCTCgTAAATCCTCATCAATCATCCAgTAAACCgCC	AAAAA	TTCAgCTCgATgCggTTCACCAgggTgTCgCCCTCgAACTTCACCTCggC	AAAAA	AgCTCAgTCCATCCTCgTAAATCCTCATCAATCATC
CCTCgTAAATCCTCATCAATCATCCAgTAAACCgCC	AAAAA	ACgCTgCCgTCCTCgATgTTgTggCggATCTTgAAgTTCACCTTgATgCC	AAAAA	AgCTCAgTCCATCCTCgTAAATCCTCATCAATCATC
CCTCgTAAATCCTCATCAATCATCCAgTAAACCgCC	AAAAA	gCgggTCTTgTAgTTgCCgTCgTCCTTgAAgAAgATggTgCgCTCCTggA	AAAAA	AgCTCAgTCCATCCTCgTAAATCCTCATCAATCATC
CCTCgTAAATCCTCATCAATCATCCAgTAAACCgCC	AAAAA	CgTAgCCTTCgggCATggCggACTTgAAgAAgTCgTgCTgCTTCATgTgg	AAAAA	AgCTCAgTCCATCCTCgTAAATCCTCATCAATCATC

Target mRNA: **tropomyosin 3 (*tpm3*)**
Amplifier: **DNA HCR B1**
Fluorophore: **Alexa Fluor 514**

Initiator I1	Spacer	Probe Sequence	Spacer	Initiator I2
gAggAgggCAgCAAACgggAAgAgTCTTCCTTTACg	ATATT	CCAgCTTTTgCAgggCTgTggCCAgTCTCTCCTgAgCACgATCCAACTCC	ATATA	gCATTCTTTCTTgAggAgggCAgCAAACgggAAgAg
gAggAgggCAgCAAACgggAAgAgTCTTCCTTTACg	ATATT	AATCACCTTCATCCCTCTCTCGCTCTCATCTGCGGCCTTCTCGGCTTCCT	ATATA	gCATTCTTTCTTgAggAgggCAgCAAACgggAAgAg
gAggAgggCAgCAAACgggAAgAgTCTTCCTTTACg	ATATT	TggATCTCCTgCAgCTCCATCTTCTCCTCATCCTTCAgAgCCCTgTTCTC	ATATA	gCATTCTTTCTTgAggAgggCAgCAAACgggAAgAg
gAggAgggCAgCAAACgggAAgAgTCTTCCTTTACg	ATATT	CTTCATATTTgCggTCAgCCTCCTCAgCAATgTgCTTggCCTCCTTAAgC	ATATA	gCATTCTTTCTTgAggAgggCAgCAAACgggAAgAg
gAggAgggCAgCAAACgggAAgAgTCTTCCTTTACg	ATATT	CTCTgTACgCTCCAACTCTCCCTCAACgATCACCAgCTTACgAgCCACCT	ATATA	gCATTCTTTCTTgAggAgggCAgCAAACgggAAgAg

Target mRNA: **ELAV (Embryonic lethal, abnormal vision, *Drosophila*)-like 3 (Hu antigen C) (*elavl3*)**
Amplifier: **DNA HCR B3**
Fluorophore: **Alexa Fluor 546**

Initiator I1	Spacer	Probe Sequence	Spacer	Initiator I2
gTCCCTgCCTCTATATCTCCACTCAACTTTAACCCg	TACAA	gCTTCgTTCCgTTTgTCgAACCgAATgAAACCTACCCCgCgCgATATACC	TAAAA	AAAgTCTAATCCgTCCCTgCCTCTATATCTCCACTC
gTCCCTgCCTCTATATCTCCACTCAACTTTAACCCg	TACAA	CTgTCCTgTCTTCTgACTggggTTgTTggCgAACTTTACggTgATgggCT	TAAAA	AAAgTCTAATCCgTCCCTgCCTCTATATCTCCACTC
gTCCCTgCCTCTATATCTCCACTCAACTTTAACCCg	TACAA	TgTCAATggTTATgggggAgAATCTgAAgCgCTgggTCTggTggTgCAgA	TAAAA	AAAgTCTAATCCgTCCCTgCCTCTATATCTCCACTC
gTCCCTgCCTCTATATCTCCACTCAACTTTAACCCg	TACAA	AggACACTTTCgTCAgCTTCCggggACAggTTgTAgACgAAgATgCACCA	TAAAA	AAAgTCTAATCCgTCCCTgCCTCTATATCTCCACTC
gTCCCTgCCTCTATATCTCCACTCAACTTTAACCCg	TACAA	ggTCATggTgACgAAgCCAAAgCCCTTACATTTgTTggTggTgAAgTCAC	TAAAA	AAAgTCTAATCCgTCCCTgCCTCTATATCTCCACTC

Target mRNA: **no tail a (*ntla*)**
Amplifier: **DNA HCR B4**
Fluorophore: **Alexa Fluor 647**

Initiator I1	Spacer	Probe Sequence	Spacer	Initiator I2
CCTCAACCTACCTCCAACTCTCACCATATTCgCTTC	TAAAA	TgTAgTTATTggTggTAgTgCTgCggTgggAgTAATggCTgggATATggA	ATTTT	CACATTTACAgACCTCAACCTACCTCCAACTCTCAC
CCTCAACCTACCTCCAACTCTCACCATATTCgCTTC	TAAAA	gTgTTTgTggTgTgggCCAgggTTCCCATCCCgCTggAgTTggggATCTg	ATTTT	CACATTTACAgACCTCAACCTACCTCCAACTCTCAC
CCTCAACCTACCTCCAACTCTCACCATATTCgCTTC	TAAAA	TgTCAggCCACCTgTAATggAgCCCgATgCTgAgCCTgATggggTgAgAg	ATTTT	CACATTTACAgACCTCAACCTACCTCCAACTCTCAC
CCTCAACCTACCTCCAACTCTCACCATATTCgCTTC	TAAAA	CCTCgCTTAggCCTggATCgTACATTgAggAgggAgAggACACAggCAgC	ATTTT	CACATTTACAgACCTCAACCTACCTCCAACTCTCAC
CCTCAACCTACCTCCAACTCTCACCATATTCgCTTC	TAAAA	TCCTTAAATgTgAAgCgATCTCAgTAgCTCTgAgCCACAggCgCCCATgA	ATTTT	CACATTTACAgACCTCAACCTACCTCCAACTCTCAC

S5.5 Probes for Figures 8 and S24

The *egfp* mRNA is redundantly detected with two probe sets containing three and five 2-initiator DNA probes. The *desm* mRNA is detected with a probe set containing three 2-initiator DNA probes. Within a given probe set, each probe initiates the same DNA HCR amplifier.

Target mRNA: **enhanced green fluorescent protein (*egfp*)**
Amplifier: **DNA HCR B1**
Fluorophore: **Alexa Fluor 514**

Initiator I1	Spacer	Probe Sequence	Spacer	Initiator I2
gAggAgggCAgCAAACgggAAgAgTCTTCCTTTACg	ATATT	gTTCTTCTgCTTgTCggCCATgATATAgACgTTgTggCTgTTgTAgTTgT	ATATA	gCATTCTTTCTTgAggAgggCAgCAAACgggAAgAg
gAggAgggCAgCAAACgggAAgAgTCTTCCTTTACg	ATATT	gTggTTgTCgggCAgCAgCACggggCCgTCgCCgATgggggTgTTCTgCT	ATATA	gCATTCTTTCTTgAggAgggCAgCAAACgggAAgAg
gAggAgggCAgCAAACgggAAgAgTCTTCCTTTACg	ATATT	gCCAgggCACgggCAgCTTgCCggTggTgCAgATgAACTTCAgggTCAgC	ATATA	gCATTCTTTCTTgAggAgggCAgCAAACgggAAgAg

Target mRNA: **enhanced green fluorescent protein (*egfp*)**
Amplifier: **DNA HCR B2**
Fluorophore: **Alexa Fluor 488**

Initiator I1	Spacer	Probe Sequence	Spacer	Initiator I2
CCTCgTAAATCCTCATCAATCATCCAgTAAACCgCC	AAAAA	TTCAgCTCgATgCggTTCACCAgggTgTCgCCCTCgAACTTCACCTCggC	AAAAA	AgCTCAgTCCATCCTCgTAAATCCTCATCAATCATC
CCTCgTAAATCCTCATCAATCATCCAgTAAACCgCC	AAAAA	ACgCTgCCgTCCTCgATgTTgTggCggATCTTgAAgTTCACCTTgATgCC	AAAAA	AgCTCAgTCCATCCTCgTAAATCCTCATCAATCATC
CCTCgTAAATCCTCATCAATCATCCAgTAAACCgCC	AAAAA	gCgggTCTTgTAgTTgCCgTCgTCCTTgAAgAAgATggTgCgCTCCTggA	AAAAA	AgCTCAgTCCATCCTCgTAAATCCTCATCAATCATC
CCTCgTAAATCCTCATCAATCATCCAgTAAACCgCC	AAAAA	CgTAgCCTTCgggCATggCggACTTgAAgAAgTCgTgCTgCTTCATgTgg	AAAAA	AgCTCAgTCCATCCTCgTAAATCCTCATCAATCATC
CCTCgTAAATCCTCATCAATCATCCAgTAAACCgCC	AAAAA	gCggTCACgAACTCCAgCAggACCATgTgATCgCgCTTCTCgTTggggTC	AAAAA	AgCTCAgTCCATCCTCgTAAATCCTCATCAATCATC

Target mRNA: **desmin (*desm*)**
Amplifier: **DNA HCR B4**
Fluorophore: **Alexa Fluor 546**

Initiator I1	Spacer	Probe Sequence	Spacer	Initiator I2
CCTCAACCTACCTCCAACTCTCACCATATTCgCTTC	TAAAA	CTTCgTgAAgACCCTCgATACgTCTTTCCAggTCCAgCCTggCCAgAgTg	ATTTT	CACATTTACAgACCTCAACCTACCTCCAACTCTCAC
CCTCAACCTACCTCCAACTCTCACCATATTCgCTTC	TAAAA	gCAgCATCgACATCAgCTCTgAAAgCAgAAAggTTgTTTTCAgCTTCCTC	ATTTT	CACATTTACAgACCTCAACCTACCTCCAACTCTCAC
CCTCAACCTACCTCCAACTCTCACCATATTCgCTTC	TAAAA	CTCACTCATTTgCCTCCTCAgAgACTCATTggTgCCCTTgAgAgAgTCAA	ATTTT	CACATTTACAgACCTCAACCTACCTCCAACTCTCAC

S6 HCR amplifier sequences

Initiator and hairpin sequences for the two RNA HCR amplifiers and five DNA HCR amplifiers used in the present work. All sequences are listed 5′ to 3′. We examine initiation of the RNA hairpins using one initiator (I1), and initiation of the DNA hairpins using one initiator (I1 or I2) or two initiators (I1 + I2).

`/5′-dye-C12/:` 5′ Alexa Fluor modification with a C12 spacer
`/C9-dye-3′/:` 3′ Alexa Fluor modification with a C9 spacer

RNA HCR A1

I1	CCgAAUACAAAgCAUCAACgACUAgA
H1	UCUAgUCgUUgAUgCUUUgUAUUCggCgACAgAUAACCgAAUACAAAgCAUC /C9-dye-3′/
H2	/5′-dye-C12/ CCgAAUACAAAgCAUCAACgACUAgAgAUgCUUUgUAUUCggUUAUCUgUCg

RNA HCR A3

I1	gACUACUgAUAACUggAUUgCCUUAg
H1	CUAAggCAAUCCAgUUAUCAgUAgUCUgACACgACUgACUACUgAUAACUgg /C9-dye-3′/
H2	/5′-dye-C12/ gACUACUgAUAACUggAUUgCCUUAgCCAgUUAUCAgUAgUCAgUCgUgUCA

DNA HCR B1

I1	gAggAgggCAgCAAACgggAAgAgTCTTCCTTTACg
I2	gCATTCTTTCTTgAggAgggCAgCAAACgggAAgAg
H1	CgTAAAggAAgACTCTTCCCgTTTgCTgCCCTCCTCgCATTCTTTCTTgAggAgggCAgCAAACgggAAgAg /C9-dye-3′/
H2	/5′-dye-C12/ gAggAgggCAgCAAACgggAAgAgTCTTCCTTTACgCTCTTCCCgTTTgCTgCCCTCCTCAAgAAAgAATgC

DNA HCR B2

I1	CCTCgTAAATCCTCATCAATCATCCAgTAAACCgCC
I2	AgCTCAgTCCATCCTCgTAAATCCTCATCAATCATC
H1	ggCggTTTACTggATgATTgATgAggATTTACgAggAgCTCAgTCCATCCTCgTAAATCCTCATCAATCATC /C9-dye-3′/
H2	/5′-dye-C12/ CCTCgTAAATCCTCATCAATCATCCAgTAAACCgCCgATgATTgATgAggATTTACgAggATggACTgAgCT

DNA HCR B3

I1	gTCCCTgCCTCTATATCTCCACTCAACTTTAACCCg
I2	AAAgTCTAATCCgTCCCTgCCTCTATATCTCCACTC
H1	CgggTTAAAgTTgAgTggAgATATAgAggCAgggACAAAgTCTAATCCgTCCCTgCCTCTATATCTCCACTC /C9-dye-3′/
H2	/5′-dye-C12/ gTCCCTgCCTCTATATCTCCACTCAACTTTAACCCggAgTggAgATATAgAggCAgggACggATTAgACTTT

DNA HCR B4

I1	CCTCAACCTACCTCCAACTCTCACCATATTCgCTTC
I2	CACATTTACAgACCTCAACCTACCTCCAACTCTCAC
H1	gAAgCgAATATggTgAgAgTTggAggTAggTTgAggCACATTTACAgACCTCAACCTACCTCCAACTCTCAC /C9-dye-3′/
H2	/5′-dye-C12/ CCTCAACCTACCTCCAACTCTCACCATATTCgCTTCgTgAgAgTTggAggTAggTTgAggTCTgTAAATgTg

DNA HCR B5

I1	CTCACTCCCAATCTCTATCTACCCTACAAATCCAAT
I2	CACTTCATATCACTCACTCCCAATCTCTATCTACCC
H1	ATTggATTTgTAgggTAgATAgAgATTgggAgTgAgCACTTCATATCACTCACTCCCAATCTCTATCTACCC /C9-dye-3′/
H2	/5′-dye-C12/ CTCACTCCCAATCTCTATCTACCCTACAAATCCAATgggTAgATAgAgATTgggAgTgAgTgATATgAAgTg

References

[1] Choi, H. M. T.; Chang, J.; Trinh, L. A.; Padilla, J.; Fraser, S. E.; Pierce, N. A. Programmable in Situ Amplification for Multiplexed Imaging of mRNA Expression. *Nat. Biotechnol.* **2010**, *28*, 1208–1212.

[2] Choi, H. M. T., *Programmable in Situ Amplification for Multiplexed Bioimaging*. Ph.D. Thesis, California Institute of Technology **2009**.

[3] Dirks, R. M.; Bois, J. S.; Schaeffer, J. M.; Winfree, E.; Pierce, N. A. Thermodynamic Analysis of Interacting Nucleic Acid Strands. *SIAM Rev.* **2007**, *49*, 65–88.

[4] Zadeh, J. N.; Steenberg, C. D.; Bois, J. S.; Wolfe, B. R.; Pierce, M. B.; Khan, A. R.; Dirks, R. M.; Pierce, N. A. NUPACK: Analysis and Design of Nucleic Acid Systems. *J. Comput. Chem.* **2011**, *32*, 170–173.

[5] SantaLucia, J., Jr. A Unified View of Polymer, Dumbbell, and Oligonucleotide DNA Nearest-Neighbor Thermodynamics. *Proc. Natl. Acad. Sci. USA* **1998**, *95*, 1460–1465.

[6] SantaLucia, J., Jr.; Hicks, D. The Thermodynamics of DNA Structural Motifs. *Annu. Rev. Biophys. Biomol. Struct.* **2004**, *33*, 415–440.

[7] Koehler, R.T.; Peyret, N. Thermodynamic Properties of DNA Sequences: Characteristic Values for the Human Genome. *Bioinformatics* **2005**, *21*, 3333–3339.

[8] Taylor, J.R. *An Introduction to Error Analysis: The Study of Uncertainties in Physical Measurements*; University Science Books: Sausalito, CA, 1997.

[9] Adler, J.; Parmryd, I. Quantifying Colocalization by Correlation: The Pearson Correlation Coefficient is Superior to the Mander's Overlap Coefficient. *Cytometry A* **2010**, *77A*, 733–742.

[10] Sprague, J.; Bayraktaroglu, L.; Clements, D.; Conlin, T.; Fashena, D.; Frazer, K.; Haendel, M.; Howe, D. G.; Mani, P.; Ramachandran, S.; Schaper, K.; Segerdell, E.; Song, P.; Sprunger, B.; Taylor, S.; Van Slyke, C. E.; Westerfield, M. The Zebrafish Information Network: The Zebrafish Model Organism Database. *Nucleic Acids Res.* **2006**, *34*, D581–D585.